

# MXene-based materials for removal of antibiotics and heavy metals from wastewater– a review

Farooque Ahmed Janjhi<sup>a,b,\*</sup>, Ihsanullah Ihsanullah<sup>c,\*\*\*</sup>, Muhammad Bilal<sup>d</sup>, Roberto Castro-Muñoz<sup>b,e,\*</sup>, Grzegorz Boczkaj<sup>b,f,\*\*\*\*</sup>, Fausto Gallucci<sup>g</sup>

<sup>a</sup> Gdansk University of Technology, Faculty of Chemistry, Department of Process Engineering and Chemical Technology, 80 – 233, Gdansk, G. Narutowicza St. 11/12, Poland

<sup>b</sup> Gdansk University of Technology, Faculty of Civil and Environmental Engineering, Department of Sanitary Engineering, 80 – 233, Gdansk, G. Narutowicza St. 11/12, Poland

<sup>c</sup> Chemical and Water Desalination Engineering Program, College of Engineering, University of Sharjah, Sharjah, 27272, United Arab Emirates

<sup>d</sup> Department of Chemical Engineering, University of Engineering and Technology, Peshawar, 25120, Pakistan

<sup>e</sup> Tecnologico de Monterrey, Campus Toluca, Av. Eduardo Monroy Cárdenas 2000 San Antonio Buenavista, 50110, Toluca de Lerdo, Mexico

<sup>f</sup> Advanced Materials Center, Gdansk University of Technology, 80 – 233, Gdansk, G. Narutowicza St. 11/12, Poland

<sup>g</sup> Sustainable Process Engineering, Chemical Engineering and Chemistry, Eindhoven University of Technology, the Netherlands

## ARTICLE INFO

### Keywords:

MXene  
2D materials  
Heavy metals  
Antibiotics  
Membranes  
Wastewater treatment

## ABSTRACT

As a novel family of 2D materials, MXenes provide an extensive variety of applications in water and effluent treatment due to their distinctive properties and attractive applicability, including superior electrical conductivity, higher thermal stability, hydrophilicity, and high sorption-reduction capacity. Their excellent sorption selectivity makes them perfect for removing hazardous contaminants. Currently, MXene-based materials are regarded as one of the most important topics in membrane separation processes. This work presents a comprehensive review of recent developments in MXene-based water treatment materials. The applications of MXene-based membranes, adsorbents, and photo-catalysts in removing antibiotics and heavy metals from water are discussed. A comparison of MXene-based membranes with other 2D membranes is outlined. Finally, prospects and challenges for future research are discussed.

## 1. Introduction

The global demand and consumption of water have increased because of the growing population, rapid urbanisation, and industrialization. Concurrently, anthropogenic activities caused high water pollution that in turn causes a significant risk to humans,

\* Corresponding author. Gdansk University of Technology, Faculty of Civil and Environmental Engineering, Department of Sanitary Engineering, 80 – 233, Gdansk, G. Narutowicza St. 11/12, Poland.

\*\* Corresponding author. Gdansk University of Technology, Faculty of Chemistry, Department of Process Engineering and Chemical Technology, 80 – 233, Gdansk, G. Narutowicza St. 11/12, Poland.

\*\*\* Corresponding author.

\*\*\*\* Corresponding author. Gdansk University of Technology, Faculty of Civil and Environmental Engineering, Department of Sanitary Engineering, 80 – 233, Gdansk, G. Narutowicza St. 11/12, Poland.

E-mail addresses: [janjhifarooque@gmail.com](mailto:janjhifarooque@gmail.com), [farooque.janjhi@pg.edu.pl](mailto:farooque.janjhi@pg.edu.pl) (F.A. Janjhi), [ihsanullah@sharjah.ac.ae](mailto:ihsanullah@sharjah.ac.ae) (I. Ihsanullah), [castromr@tec.mx](mailto:castromr@tec.mx), [food.biotechnology88@gmail.com](mailto:food.biotechnology88@gmail.com), [roberto.castro-munoz@pg.edu.pl](mailto:roberto.castro-munoz@pg.edu.pl) (R. Castro-Muñoz), [grzegorz.boczkaj@pg.edu.pl](mailto:grzegorz.boczkaj@pg.edu.pl) (G. Boczkaj).

<https://doi.org/10.1016/j.wri.2023.100202>

Received 19 September 2022; Received in revised form 30 January 2023; Accepted 1 February 2023

Available online 2 February 2023

2212-3717/© 2023 The Authors. Published by Elsevier B.V. This is an open access article under the CC BY-NC-ND license (<http://creativecommons.org/licenses/by-nc-nd/4.0/>).

aquatic life, and the ecosystem [1,2]. Different pollutants exist in various industrial effluents and may vary depending on the manufacturing company and other processing industries [3]. Mining, steel/iron production, oil/gas fracking, industrial laundries, powerhouse, metal finishers, and the food/beverage industries are all responsible for the release of the enormous amount of contaminated wastewater. Numerous contaminants, including toxins, heavy metals, oils, pesticide residues, sludge, medical products, as well as other industrial by-products, can be found in municipal and industrial water outlets [4–6].

A large number of pharmaceutically active compounds (PhACs) have been released into the environment without being properly treated over the past two decades [1]. Antibiotics are a very dangerous type of such compounds that cause contamination of the aqueous environment. Several antibiotics such as fluoroquinolones, lincomycin, sulfonamides, and tetracyclines are widely used in livestock farming, pharmaceuticals, and chicken metabolic products to cure and treat microbial infectious diseases [7]. Overuse of these pollutants and their untreated discharge cause environmental problems.

In a similar way, other highly harmful elements (such as toxic metal ions) also have a tendency to bio-accumulate and can slowly release into waterways, posing significant risks to aquatic life. Mining, recovery, and other commercial operations that involve multiple toxic metal ions ( $Zn^{2+}$ ,  $Cd^{2+}$ ,  $Pb^{2+}$ ,  $Cr^{6+}$ , and  $Cu^{2+}$ ) are common sources of wastewater discharge that can eventually reach natural water bodies [8–11]. Rapid industrialization caused the mobilization of heavy metals into the environment, which is a major concern due to their toxicity, and therefore, these lethal ions had a drastic effect on the ecosystems, human health, and other living organisms [12]. Thus, eliminating such lethal pollutants from an aqueous environment is considered indispensable to preserving the ecosystem and human life.

Literature reported the application of various treatment techniques in eliminating contaminants/pollutants from wastewater, such as *adsorption* [12–18], *advanced oxidation* [19–22], *membrane separation* [23–28], *ozonation* [29,30], *ion exchange* [31], *chemical precipitation* [32], *electro-dialysis* [33], *photo-catalytic degradation* [34–38], *bio-surfactants* [39], *electrocoagulation* [40], and other physical, chemical, and biological treatment methods [29,41–44]. Most of these treatment techniques have certain drawbacks in treating wastewater including complex removal mechanisms, disposal challenges, excessive use of chemicals, generation of sludge and by-products, high energy consumption, insufficient removal of noxious compounds, not being valuable at very low concentrations of

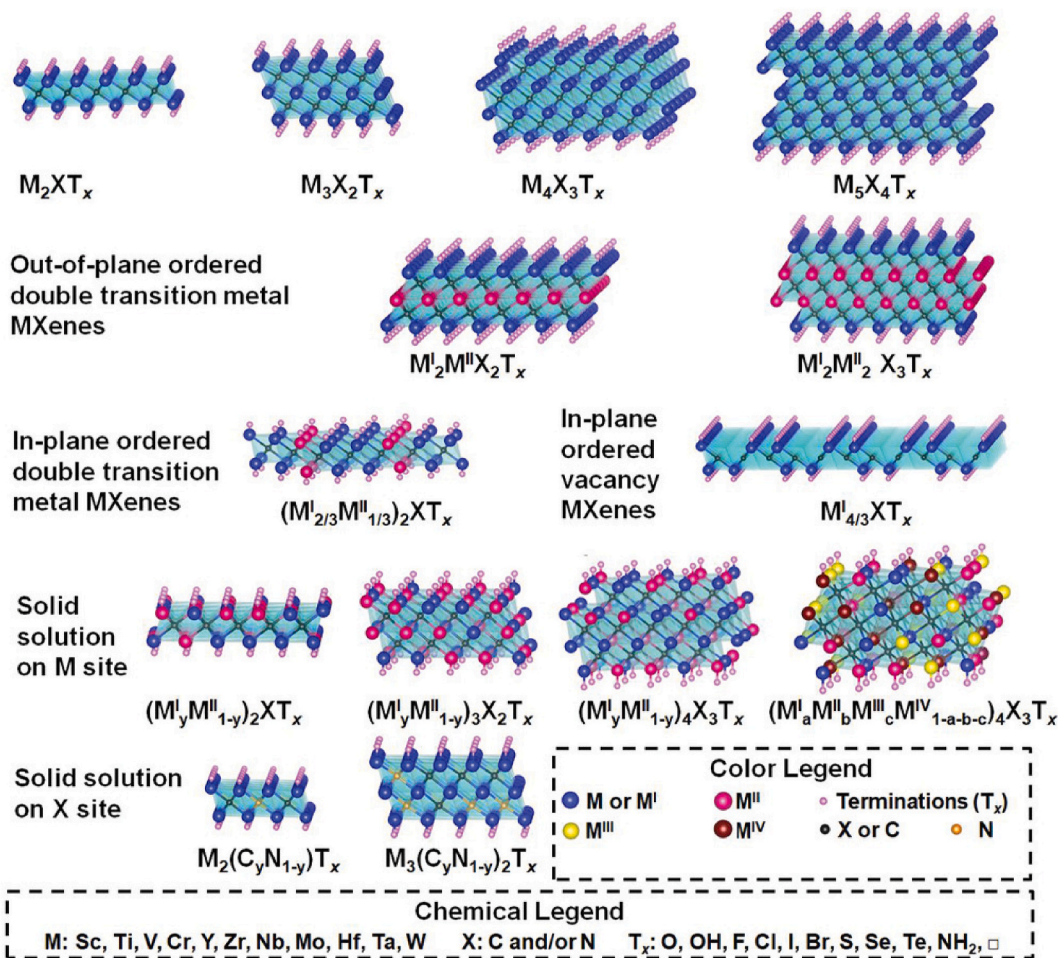


Fig. 1. Typical MXene structures and compositions. Reprinted with permission from Ref. [68]. Copyright (2021), Wiley-VCH GmbH.

contaminants, formation of toxic by-products, and regeneration ability [45]. In a similar way, the photo-catalysis processes which employed n-type semiconductors ( $\text{TiO}_2$ ) are eco-friendly, with fascinating potential in removing stable organic contaminants because of the degradation and mineralization of the organic pollutants [46]. However, the employed semiconductors like  $\text{TiO}_2$  often failed to be witnessed under visible light illumination. This is ascribed to the high electron/hole ( $e^-/h^+$ ) pair recombination rate and higher band gap ( $\sim 3.2$  eV) [47]. Other semiconductor materials like transition metal sulphides also had the disadvantage of photo-corrosion which is the self-oxidation of photo-induced holes [48]. Such drawbacks can easily be avoided by developing a heterogeneous Z-type system comprised of a potent electron-donor semiconductor [48–50].

Recently, a number of nanocomposites have displayed remarkable potential in water purification owing to their incredible physicochemical features [51–55]. Membrane-based wastewater treatment methods have found incredible consideration in recent times. Numerous 2D materials such as covalent organic frameworks (COFs), graphene oxide (GO) [56], layered zeolites [57,58], metal-organic frameworks (MOFs) [59], and transition metal dichalcogenides (TMDs) have been widely applied for membrane synthesis with superior separation performances [60–62]. MXenes, on the other hand, are a new family of 2D nanomaterials, discovered by Drexel University researchers in 2011 [63,64]. MXenes are usually described by the formula  $\text{M}_{n+1}\text{X}_n\text{T}_x$ , where M is an early transition metal like Ti, Mo, Sc, W, V, or Zr; X is carbon or nitrogen; T represents the surface termination group like  $-\text{Cl}$ ,  $-\text{F}$ ,  $=\text{O}$ , or  $-\text{OH}$ ; x is the number of surface functional groups; and n ranges from 1 to 4 [65–67]. Typical MXene structures and compositions are illustrated in Fig. 1 [68].

These new class of materials (MXenes) are a good alternative to many applications because of their unique structural features such as ease of fabrication, hydrophilicity, considerable interlayer spacing, dynamic electrochemistry, activated metallic hydroxide sites, high specific surface area, higher conductivity, biocompatibility, incredible chemical stability, ion exchange property, maximum chemical stability, robust surface functional groups, and superior adsorption-reduction capability [69–73]. These materials have been at the forefront of studies for developing MXene-based membranes and photo-catalysts in removing/degrading various contaminants and different pollutants from wastewater [69,74–76].

This review focuses on the latest advances and novelties in MXene-based membranes and materials (adsorbents and photo-catalysts) for the removal of heavy metals and antibiotics from wastewater. The effectiveness of various MXene-based membranes at removing harmful pollutants is carefully assessed and the applications of MXenes as adsorbents and photo-catalysts are described in considerable detail. Moreover, a comparative analysis of the MXene membranes with other 2D materials is also provided. Lastly, various intended challenges are highlighted and recommendations regarding future research are provided.

## 2. Removal of heavy metals and antibiotics by MXene-based membranes

### 2.1. Removal of heavy metals

MXenes have been employed for the removal of various heavy metals from the aqueous phase, such as copper ( $\text{Cu}^{2+}$ ), chromium ( $\text{Cr}^{6+}$ ), barium ( $\text{Ba}^{2+}$ ), cadmium ( $\text{Cd}^{2+}$ ), mercury ( $\text{Hg}^{2+}$ ), and lead ( $\text{Pb}^{2+}$ ). Considering that heavy metal ions possess a size lower than  $4.5 \text{ \AA}$ , they can be easily entrapped within the interlayer spacing (lower than  $2 \text{ \AA}$ ) of MXene sheets. Apart from this, the chemical functionalities of the MXene's surface are also responsible to display an enhanced adsorptive uptake. MXene-based membranes have emerged as novel membranes for the uptake of heavy metal ions from water [77]. A summary of published literature on the applications of MXene-based membranes for the removal of metal ions is presented in Table 1.

Xie et al. (2019) employed  $\text{Ti}_3\text{C}_2\text{T}_x$ -based membranes by intercalating reduced graphene oxide between the layers [83]. Nanomaterials were successfully incorporated into the membrane by hydroxylation, which led to increased wettability, adsorption ability, and metal ions reduction. Experimentally, only 44% of the initial  $\text{Cr}(\text{VI})$  was removed after 150 min over the pristine  $\text{Ti}_3\text{C}_2\text{T}_x$  membrane, which was mainly ascribed to its dense configuration that restricted the mass transfer of  $\text{HCrO}_4^-$ , while the performance of  $\text{HCrO}_4^-$  removal of the composite membrane resulted as high as 91% after 150 min. Interestingly, the authors reported that after  $\text{HCrO}_4^-$

**Table 1**  
Metal ions removal/recovery by MXene-based membranes.

Mxene-based membranes	Metal ions	Water permeability ( $\text{L m}^{-2} \text{ h}^{-1} \text{ bar}^{-1}$ )	Separation/rejection efficiency (%)	Reference
PFDTMS-modified hydrophobic 2D d- $\text{Ti}_3\text{C}_2$ membrane	$\text{Cu}^{2+}$ $\text{Cr}^{6+}$	–	$\sim 100$ –	[78]
Mxene-anchored goethite heterogeneous Fenton composite ( $\beta\text{-FeOOH@Mxene}_{0.2}$ ) freestanding membrane	$\text{Hg}^{2+}$	–	99.7	[79]
Thermal cross-linked 2D Mxene ( $\text{Ti}_2\text{C}_3\text{T}_x$ ) membrane	$\text{Pb}^{2+}$	$\sim 250 \text{ L/m}^2\cdot\text{h}$	Hydrated rejection of $\text{Pb}^{2+}$ : 99-	[80]
$\text{Ti}_3\text{C}_2\text{T}_x$ Mxene@MOF decorated polyvinylidene fluoride membrane	$\text{Ni}^{2+}$ $\text{Cd}^{2+}$ $\text{Mn}^{2+}$ $\text{Cu}^{2+}$ $\text{Zn}^{2+}$	$17.1 \pm 0.2$	$>95.2 \pm 0.5$ $95.2 \pm 0.5$ $97.6 \pm 0.4$ $95.2 \pm 0.5$ $95.2 \pm 0.5$	[81]
Mxene ( $\text{Ti}_3\text{C}_2\text{T}_x$ ) membrane	$\text{Pb}^{2+}$ $\text{Cu}^{2+}$ $\text{Cd}^{2+}$	–	99.5 99.7 99.8	[82]

removal, a shift of 0.1–0.2 eV to greater binding energy was noted for the C-Ti<sup>δ+</sup>-T<sub>x</sub> moieties, suggesting that electrons are being drained from Ti<sub>3</sub>C<sub>2</sub>T<sub>x</sub> as it reductively removes HCrO<sub>4</sub><sup>-</sup>. In consequence, it was also considered that HCrO<sub>4</sub><sup>-</sup> elimination over Ti<sub>3</sub>C<sub>2</sub>T<sub>x</sub> follows an independent pathway of electron transfer from Ti<sub>3</sub>C<sub>2</sub>T<sub>x</sub> to HCrO<sub>4</sub><sup>-</sup>, releasing Cr(III) that can be attached in Ti<sub>3</sub>C<sub>2</sub>T<sub>x</sub>-based membranes [83].

A recent study reported an improved Be(II) removal from Be(NH<sub>2</sub>)<sub>2</sub> complexing solutions using a sandwiched Ti<sub>3</sub>C<sub>2</sub>T<sub>x</sub> MXene/nano zero-valent iron (nZVI)/fungal hypha (FH) nanofiber hybrid membrane [84]. Fig. 2a graphically illustrates the schematic for the self-assembly nanofiber preparation [84]. There were numerous MXene/nZVI catalytic units coated on the surface of the final nanofiber membranes. In high magnification, nZVI appeared to be uniformly dispersed within the MXene nanosheet layer. When dealing with water permeability, such nanofibers exhibited about 301 times greater permeability compared to bare Ti<sub>3</sub>C<sub>2</sub>T<sub>x</sub> membrane, while capturing up to 99.8% Be<sup>2+</sup> from the Be(NH<sub>2</sub>)<sub>2</sub> solution with low concentration (19.85 ppm). In particular, the best Be<sup>2+</sup> adsorption capacity of the membrane was estimated to be as high as 95.20 mg g<sup>-1</sup> at pH 5.0 and 35 °C. Based on the complete characterization of the studied membranes, Be<sup>2+</sup> forms BeO and BeO<sub>2</sub>-bidentate inner-sphere complexes on MXene nanosheets, and this contributes to efficient Be<sup>2+</sup> removal. Due to its sandwiched structure, MXene/nZVI@FH was easily activated and reused after leaching with 0.1 M HCl solution. The economic and environmental implications of this aspect are significant.

Fig. 2b shows the schematic of the synthesis of Ti<sub>3</sub>C<sub>2</sub>T<sub>x</sub> MXene@MOF@PVDF nanocomposite membranes [81]. The prepared membranes exhibited excellent removal for selected heavy metals with a rejection rate higher than 95.2 ± 0.5% for each ion, notably high for Mn<sup>2+</sup> (97.6 ± 0.4%), as depicted in Fig. 2c and d [81].

Using polyethylenimine (PEI) polymer crosslinked with dopamine and graphene oxide on the top surface of the membranes, Zhao et al. (2021) observed a decrease in the water inlet pores [85]. Consequently, the resulting GO/MXene\_PEI membranes displayed less permeance of water. In contrast, the water permeability of GO/MXene\_PEI membranes increased with decreasing load, for instance, when the membranes' load was 166 mg m<sup>-2</sup>, the membrane permeability was approximately 1.3 ± 0.1 L m<sup>-2</sup> h<sup>-1</sup> bar<sup>-1</sup>. Water permeability increased by about 3 times with a reduced membrane load of 100 mg m<sup>-2</sup>, while rejection for Ca<sup>2+</sup> and Mg<sup>2+</sup> increased slightly, but still was over 70% [85,86].

Due to the weakened adsorption associated with the reduction of negative charge during thermal self-crosslinking of MXene membranes, Wang et al. (2021) reported the regeneration of the surface charge via hydroxylation [82]. In this process, the alkali solution of KOH is used to replace -F with -OH. Surprisingly, the rejection efficiency of a 383 nm-thick hydroxylated MXene membrane was higher compared to a pristine MXene membrane when two selective membranes were used to remove Cd<sup>2+</sup>, Cu<sup>2+</sup>, and Pb<sup>2+</sup>

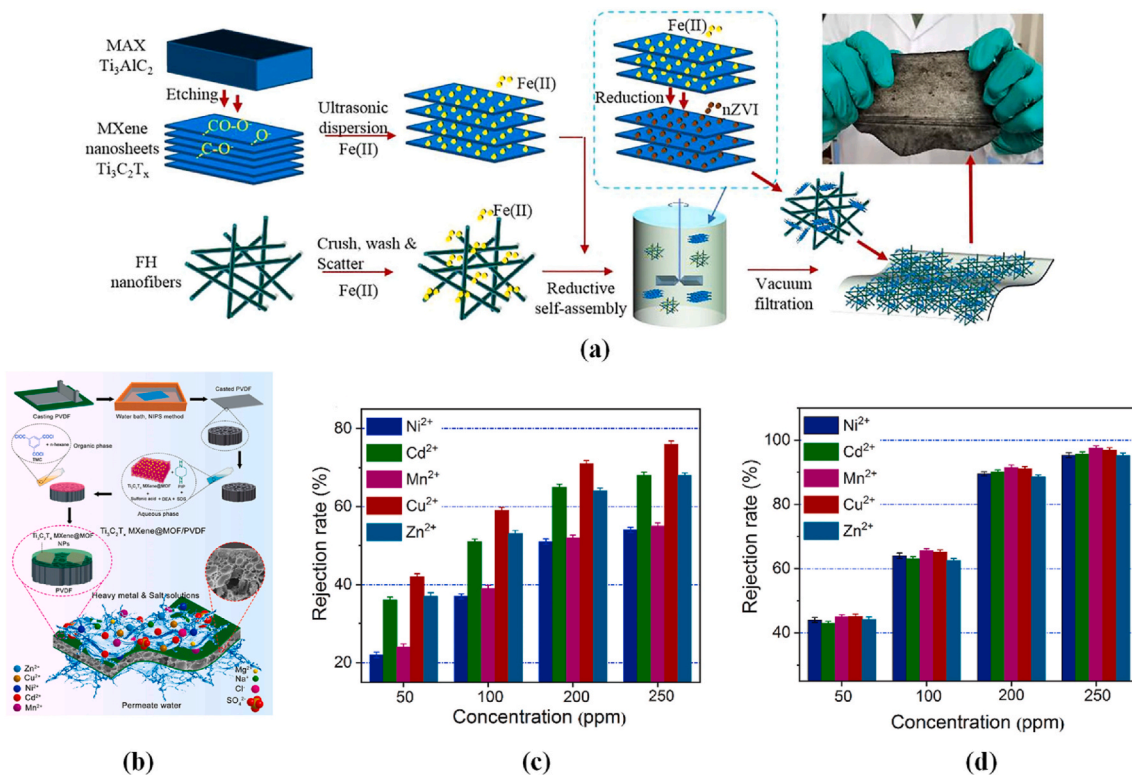


**Fig. 2.** (a) Schematic illustration of the self-assembly synthesis of MXene/nZVI@FH. Reprinted with permission from Ref. [84]. Copyright (2021), Elsevier B.V., (b) A schematic of the fabrication of thin-film composite membranes with the incorporation of synthesized Ti<sub>3</sub>C<sub>2</sub>T<sub>x</sub> MXene@MOF into the thin-film PVDF membrane. Heavy metals rejection rate for M<sub>3</sub> MXene@MOF@PVDF nanocomposite membrane with (c) 0.00 wt% (d) 0.10 wt% of Ti<sub>3</sub>C<sub>2</sub>T<sub>x</sub> MXene@MOF nanocomposite. Reprinted with permission from Ref. [81], Copyright (2022), Elsevier Ltd.

co-existing anions ( $\text{Cl}^-$  and/or  $\text{NO}_3^-$ ), under external voltage. Up to 70 min of tests, the authors concluded that, when the interlayer spacing is controlled through a thermal self-linking protocol, good operational durability and reproducibility are possible [82]. Actually, the control of the d-spacing is an important matter in terms of water treatment applications. In fact, the nanostructure of MXene, particularly the d-spacing, should be further studied, as the permeation of water molecules can cause channel enlargement in 2D materials that in turn caused influenced the rejection efficiency [87]. It was recently demonstrated that d-spacing affects the ion selectivity of MXene membranes [88].

Fan et al. (2020) reported the synthesis of MXene/PVDF membrane and evaluated its potential in the separation and removal of  $\text{K}^+$ / $\text{Pb}^{2+}$  ions by exerting external voltage, as depicted in Fig. 3 [89]. The addition of MXenes enhanced the lead ions rejection in addition to improving the anti-swelling potential of the resultant membranes.

The membrane reusability by using HCl has been also proved by Yang et al. (2020), who reported ions removal of 63, 64 and 70% for  $\text{Cu}^{2+}$ ,  $\text{Cd}^{2+}$ , and  $\text{Cr}^{6+}$ , respectively, from wastewater using  $\text{Fe}_3\text{O}_4$ @MXene composite nanofiltration membrane [8].

## 2.2. Removal of antibiotics by MXene-based membranes

In recent years, the release of antibiotics in groundwater from various effluent and clinical waste from hospitals and pharmacies has become a growing environmental concern, thus severely affecting biodiversity and other public health services [90,91]. These toxic compounds are very harmful to the ecosystem even at trace concentrations, causing the emergence of terrible viruses and bacteria with exceptionally high resistance to existing antibiotics [92]. Aquatic organisms are particularly vulnerable to some antibiotics [93]. Therefore, efficient and enhanced removal of antibiotics from an aqueous environment is a necessary step in adopting a sustainable environment.

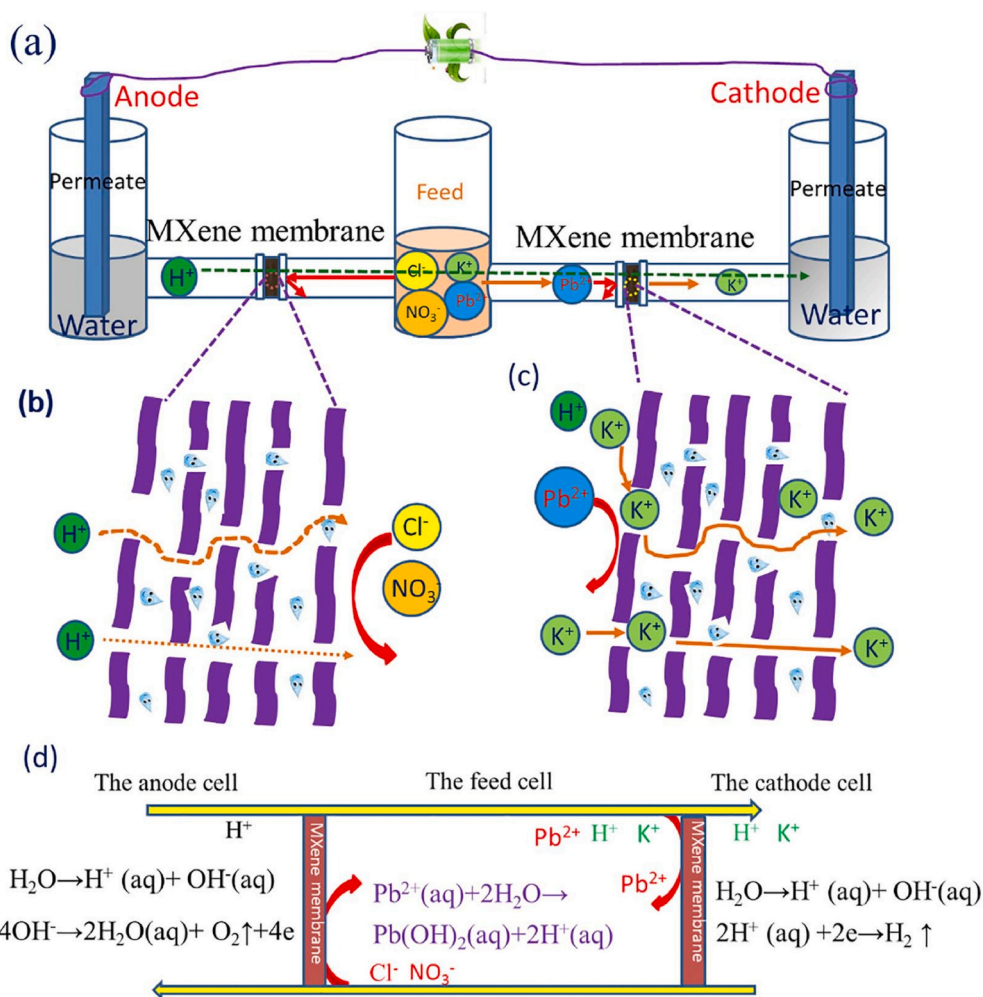


**Fig. 3.** Schematic illustration of the ion sieving mechanism induced by electric field. (a) Assembling of MXene/PVDF membrane between three cells (feed and permeate) under electric field; (b) and (c) Mechanisms of ion sieving; (d) The reactions and ion transport. Reprinted with permission from Ref. [89]. Copyright (2020), Elsevier B.V.

Nanofiltration with polymeric membranes is emerged as a potential technology, owing to its high performance, and continuous and easy operation [94–96]. Membrane fouling by the adsorption of the antibiotic is the main drawback, which decreases water permeability and membrane stability. The primary reason for membrane fouling is the electrostatic attraction between the membrane surface and the target antibiotic molecules [97]. Furthermore, the uneven pores configuration in polymeric nanofiltration membranes makes it necessary to affect the water/solvent permeation to achieve enough antibiotics rejection [95]. These deficiencies may be overcome by improving the anti-fouling resistance and regular pore structure of the employed membranes. The 2D laminated membranes exhibited better permeance and pollutants rejection via ion sieving and are good in pervaporation filtration [98,99].

The trade-off between the permeance and the selectivity in polymeric membranes can be overcome by using the  $\text{Ti}_3\text{C}_2\text{T}_x$  nanosheets with regular slit-shaped interlayer distances, which also boosted the selective permeability of the employed membranes [100,101]. Table 2 enlists various MXene-based membranes and their successful application in the removal of a range of antibiotics such as azithromycin, bacitracin, tetracycline, erythromycin, penicillin, rifampicin, and chloramphenicol (both water and alcohol soluble). The studied membranes showed effective filtration and exceptional rejection performance due to their regular spacings, equidistant nanolayers, and large aspect ratio.

Titanium carbide-based membranes have a greater solvent permeance compared to polymeric nanofiltration membranes because these have a high aspect ratio, which results in a regular two-dimensional (2D) structure and high permeation flux. Besides, the increased antifouling is also caused by the interaction between the surface terminations of the employed membranes and the target antibiotics that affect the final rejection performance of the employed membranes.

Fig. 4a provides the comparative approach between the permeability of the  $\text{Ti}_3\text{C}_2\text{T}_x$  membranes at different membrane thicknesses against the separation of tetracycline aqueous solutions [102]. Generally, membranes with greater thickness offer enhanced rejection performance compared to lower thicknesses because of the fewer defects [103]. Fig. 4b and c shows exceptional separation performance of the  $\text{Ti}_3\text{C}_2\text{T}_x$  membranes (2–4  $\mu\text{m}$  titanium carbide nanosheets) against different antibiotics (penicillin, tetracycline, azithromycin, erythromycin, bacitracin, chloramphenicol, and rifampicin) in both aqueous and ethanolic solutions [102]. The reported water permeance of the smallest penicillin molecule, with a size of 1.4 nm  $\times$  0.7 nm, was about  $223.1 \pm 9.5 \text{ L m}^{-2} \text{ h}^{-1} \text{ bar}^{-1}$ , with 89.5  $\pm$  0.5% rejection. The reported water permeability values for tetracycline, erythromycin, azithromycin, and bacitracin aqueous solutions via a 500 nm thick  $\text{Ti}_3\text{C}_2\text{T}_x$  membrane were  $250.4 \pm 5.2$ ,  $278.5 \pm 10.5$ ,  $280.4 \pm 15.2$ , and  $340.5 \pm 20.5 \text{ L m}^{-2} \text{ h}^{-1} \text{ bar}^{-1}$ , respectively. In a similar way, the rejection rates of these antibiotics in an aqueous environment are reported to be about 91.5  $\pm$  0.4%, 95  $\pm$  1.2%, 95.1  $\pm$  1.6%, and 99.5  $\pm$  0.4%, respectively. Furthermore, the  $\text{Ti}_3\text{C}_2\text{T}_x$  membrane exhibits superior separation performance of the molecular sieving for the ethanol-soluble antibiotics (rifampicin and chloramphenicol). The permeability of ethanol is specifically reported to be about  $200.5 \pm 10.2 \text{ L m}^{-2} \text{ h}^{-1} \text{ bar}^{-1}$ , with an 89.5  $\pm$  0.3% chloramphenicol rejection (1.7 nm  $\times$  1.0 nm). Similarly, the same membrane revealed 96.2  $\pm$  1.8% and  $300.5 \pm 10.2 \text{ L m}^{-2} \text{ h}^{-1} \text{ bar}^{-1}$  of ethanol rejection and permeance for the larger rifampicin molecules [102]. Fig. 4d shows the stability of the  $\text{Ti}_3\text{C}_2\text{T}_x$  membranes and their time-dependent separation performance with tetracycline aqueous solution and rifampicin ethanol solution [102]. Besides, the selectivity of the membrane could also be enhanced by carefully controlling the interlayer spacing [104].

Fig. 5 illustrates the removal mechanism of tetracycline hydrochloride (TC) from wastewater by the g- $\text{C}_3\text{N}_4$ @MXene/PES (CN-MX) composite membrane, which exhibited high permeance of  $1790 \text{ L m}^{-2} \text{ h}^{-1} \text{ bar}^{-1}$  compared to pristine MXene membrane [105]. The rejection efficiency of 86% for TC antibiotic was reported by the employed membrane. Literature also reported the superior anti-swelling characteristics of the MXene/carboxylated cellulose nanofibers ( $\text{Ti}_3\text{C}_2\text{T}_x$ /CNFs)-based membranes in a water environment, for up to 76 h [106]. The employed membrane unveiled better separation performance with high pure water permeability of  $\sim 26.0 \text{ L m}^{-2} \text{ h}^{-1} \text{ bar}^{-1}$  and high selectivity rejection of antibiotics ( $\sim 99.0\%$  for azithromycin) [106].

### 3. MXene-based materials in other water treatment applications

#### 3.1. MXenes as adsorbents for the removal of antibiotics and heavy metals

The presence of toxic heavy metal ions even in trace amounts has a drastic influence on living organisms and the environment;

**Table 2**  
Antibiotics removal by MXene-based membranes.

MXene-based membranes	Antibiotics	Water permeability ( $\text{L m}^{-2} \text{ h}^{-1} \text{ bar}^{-1}$ )	Rejection (%)	Molecular weight (g/mol)	Mechanism	Reference
$\text{Ti}_3\text{C}_2\text{T}_x$	Erythromycin	$278.5 \pm 10.5$	$95 \pm 1.2$	734	Molecular sieving and electrostatic repulsion	[102]
	Azithromycin	$280.4 \pm 15.2$	$95.1 \pm 1.6$	749		
	Tetracycline Penicillin	$250.4 \pm 5.2$	$91.5 \pm 0.4$	444.4		
	Bacitracin	$223.1 \pm 9.5$	$89.5 \pm 0.5$	334.4		
	Chloramphenicol	$340.5 \pm 20.5$	$99.5 \pm 0.4$	1422		
	Rifampicin	$200.5 \pm 10.2$	$89.5 \pm 0.3$	323		
g- $\text{C}_3\text{N}_4$ @MXene (CN-MX)	Tetracycline hydrochloride (TC)	1790	86	481	Molecular sieving and electrostatic repulsion	[105]
	$\text{Ti}_3\text{C}_2\text{T}_x$ /CNFs (carboxylated cellulose nanofibers)	26.0	$\sim 99.0\%$	749		

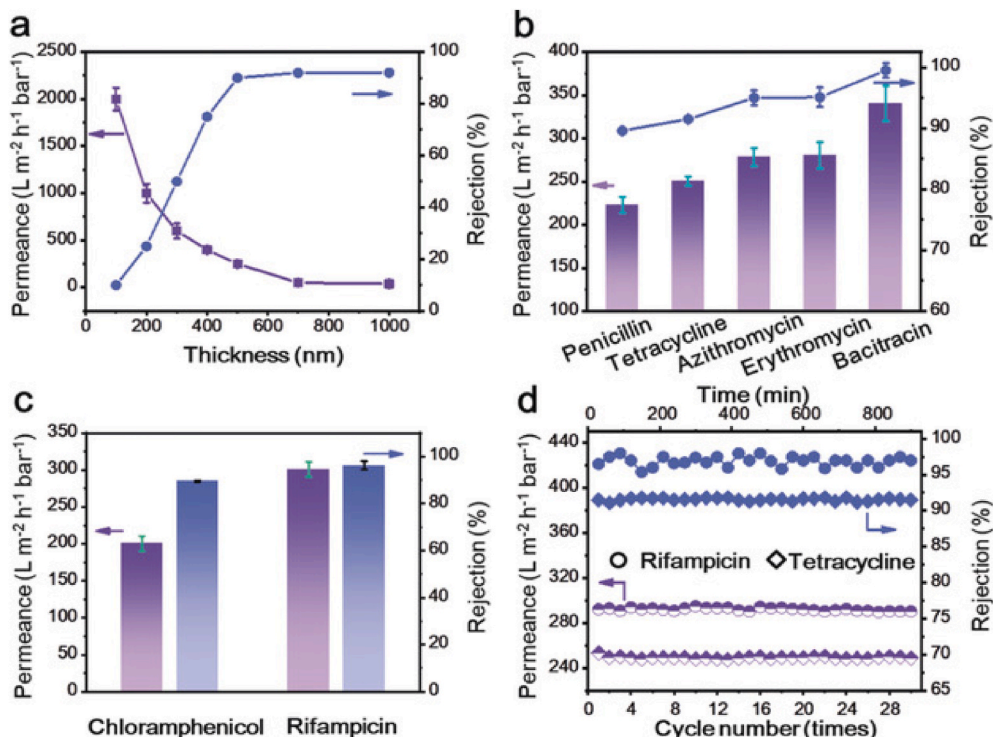


**Fig. 4.** Antibiotics separation performance of Ti<sub>3</sub>C<sub>2</sub>T<sub>x</sub> membrane, (a) Ti<sub>3</sub>C<sub>2</sub>T<sub>x</sub> membrane thickness dependent separation performance of tetracycline solution at pH 7 with feed concentration of 250 ppm in water, (b) Antibiotics separation performance for 250 ppm aqueous solution, (c) Rifampicin and chloramphenicol separation performance in ethanol solution, (d) Time dependent separation performance of Ti<sub>3</sub>C<sub>2</sub>T<sub>x</sub> membranes with tetracycline aqueous solution and rifampicin ethanol solution. Reprinted with permission from Ref. [102]. Copyright (2020), Wiley-VCH Verlag GmbH & Co. KGaA, Weinheim.

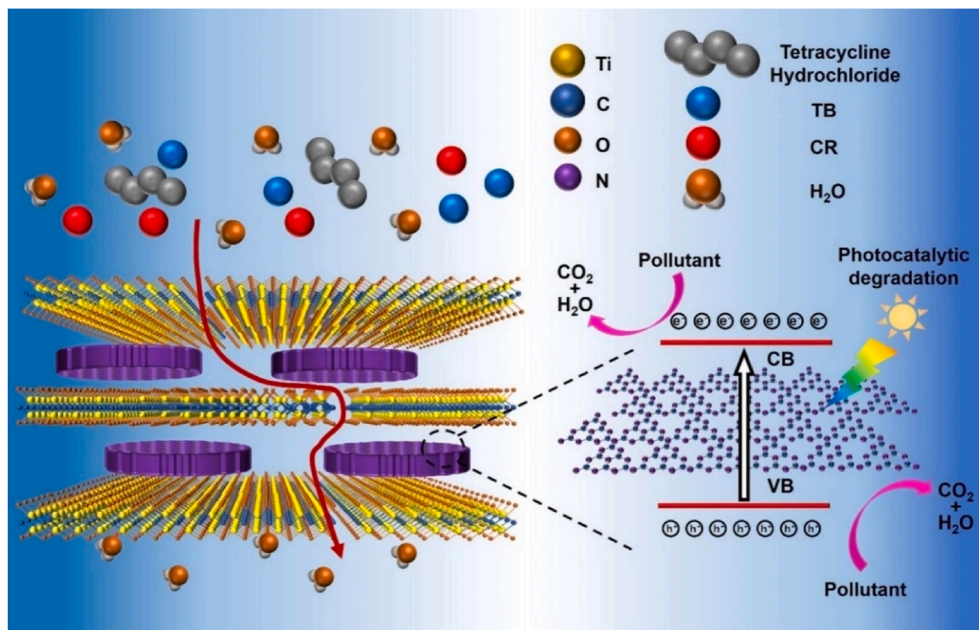


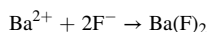
**Fig. 5.** The removal mechanism of g-C<sub>3</sub>N<sub>4</sub>@MXene/PES (CN-MX) composite membrane for dyes and antibiotics from wastewater. Reprinted with permission from Ref. [105]. Copyright (2022), Elsevier B.V.

therefore, the elimination of these lethal pollutants from the aqueous phase is an essential step in treating toxic effluents. MXenes are an ideal candidate to be employed as adsorbents material for the enhanced uptake of various heavy metal ions from an aqueous environment since they exhibit unique physicochemical and structural characteristics, such as numerous surface terminations, large specific surface area, hydrophilicity, and electron-richness [107]. These adsorbents unveiled exceptional adsorption potentials for the successful elimination of heavy metal ions from an aqueous environment [94–96]. Numerous available functional groups and active sites for adsorption on the surfaces of the employed nanomaterials also contribute to the enhanced removal of toxic heavy metals [111].

Similar to the elimination of the heavy metals, the MXene adsorbents have also revealed outstanding uptake performance for the confiscation of potentially toxic antibiotics from the water environment.

MXenes hold numerous active surface functional groups, whose activity can be significantly increased under the action of the magnetic field, and it is more evident with acidic functional groups [15]. Literature explained the development of the sodium alginate/MXene/CoFe<sub>2</sub>O<sub>4</sub> (SA/MX/CFO) composite material for the successful adsorption of Cu<sup>2+</sup> and ciprofloxacin (CIP) with an external magnetic field [15]. The adsorption potential was reported to enhance by 3.53% and 24.19% against the selective removal of Cu<sup>2+</sup> and CIP when the employed adsorbent is subjected to the rotating magnetic field (RMF). The enhancement in adsorption potential with the help of RMF is ascribed to the following reasons: (i) RMF could enhance the H-bonding of the adsorbent surface that caused an exceptional rise in CIP uptake, (ii) the energy of the magnetic field is adsorbed by the target contaminants, thus enhancing their kinetic energy and mass transfer capability, and (iii) the CFO exhibit greater strength of the magnetic field at the micro-interface compared to Fe<sub>3</sub>O<sub>4</sub>, causing higher influence of the magnetic field for both (pollutants and solutions) [15].

Fig. 6 illustrates the mechanism of barium ions uptake by the surface of the MXene layers in which both the physisorption and chemisorption are responsible for the Ba-adsorption [112]. The MXene surface is generally terminated by the –O, –OH, and –F functional groups after the etching process; therefore, these existing functional groups act as vacant active adsorption sites for Ba-ions to be adsorbed onto the adsorbent surface. The adsorption of Ba-ions by the MXene's surface functional groups occurs by the following reactions to form Ba(OH)<sub>2</sub> and Ba(F)<sub>2</sub>:



Such developed barium hydroxides and barium fluorides are the key Ba-constituent in an aqueous environment and they are chemisorbed onto the MXene surface.

Literature also reported the removal of a range of pharmaceutical compounds (amitriptyline (AMT), verapamil, carbamazepine, 17  $\alpha$ -ethinyl estradiol, ibuprofen, and diclofenac) by the sonicated Ti<sub>3</sub>C<sub>2</sub>T<sub>x</sub> MXene [113]. The highest selective adsorption was reported for the AMT, with an adsorption capacity of 58.7 mg g<sup>-1</sup> which is due to the electrostatic attraction between the positive AMT molecules and the negative MXene surface. The enhanced adsorption of the sonicated MXene compared to pristine MXene material is due to the creation of larger cavitation bubbles at lower frequencies that formed oxygenated functional groups on the MXene surface and also make well-dispersed MXene.

Another study reported the adsorption of CIP by the alkaline intercalated MXene (sodium ions (SI)–Ti<sub>3</sub>C<sub>2</sub>T<sub>x</sub>) and observed better adsorption performance compared to pristine MXene due to its high specific surface area and the broad layers (layered spacing and

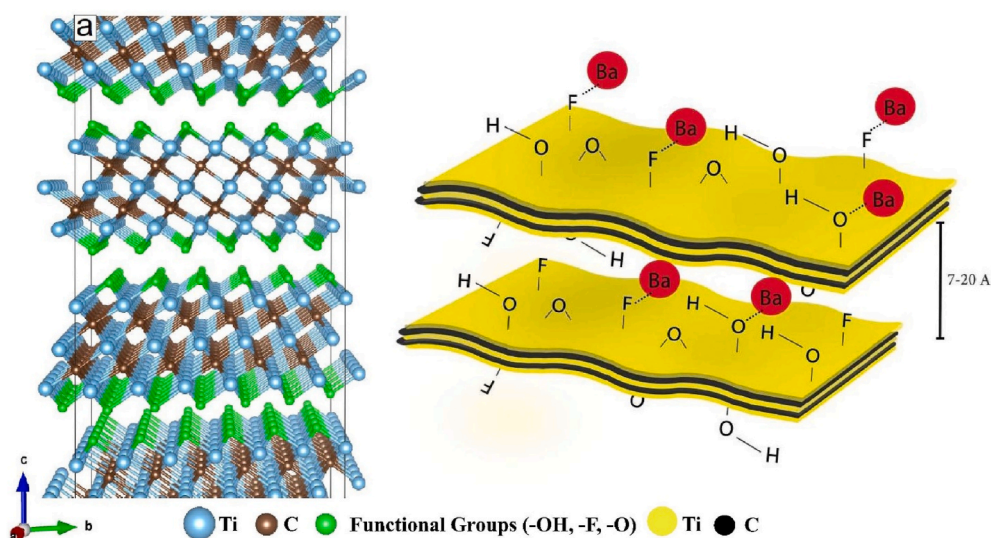


Fig. 6. Adsorption mechanism of barium ion on surface of MXene layers. Reprinted with permission from Ref. [112]. Copyright (2017), Elsevier B.V.



vacant sites) in which the pollutant molecules might be able to adsorb easily [114]. Besides, the intercalation also caused more –O and –OH surface terminations to develop on the adsorbent surface which acts as active sites for CIP adsorption. In addition, the adsorbent efficiency was also reported to marginally improved in succeeding regeneration stages (~99.7%) because of the nanosheets' crystallinity loss (enhancing amorphosity) that in turn caused increased porosity and moieties, hence resulting in the development of numerous active sites (increasing specific surface area) [114].

Table 3 and Table 4 enlist various MXene-based adsorbents and their successful applications in the removal of different heavy metal ions and antibiotics from an aqueous environment. MXene-based adsorbents unveiled enhanced adsorption potential against the elimination of antibiotics and toxic heavy metals in water treatment technologies. These studies proposed the efficient employment of MXene-based adsorbents in removing lethal contaminants and pollutants from an aqueous environment.

### 3.2. MXenes as photo-catalysts for degradation of antibiotics

Photo-catalysis is regarded as one of the cost-effective methods for the removal of various environmental contaminants [75,125,126]. MXenes, so far, have been employed in various photo-catalytic applications such as N<sub>2</sub> fixation [126–128], CO<sub>2</sub> reduction [129–132], degradation of several pollutants [127,133–135], and water splitting [136–139]. MXene could also improve the photo-catalytic activity of the as-developed composite in these applications by performing numerous functions, including limiting the size of the photo-catalyst, enhancing reactant adsorption, acting as robust support, and promoting photo-generated charge carrier separation [140].

The successful use of MXenes in photo-catalysis can be attributed primarily to the following factors: (i) developing intimate contact interfaces between the MXene and other semiconductor materials and is facilitated by numerous available functional groups, (ii) changing the surface chemistry caused by changing the bandgap alignment of the MXene, and (iii) MXene has outstanding metallic conductivity and electron acceptance due to the conductive metallic core in its layered structure [141].

In particular, MXenes can be made hybridized with other substances like polymers, graphene, MOFs etc. To enhance their photo-catalytic characteristics. MXenes with distinct lamellar structures and high conductivity have been employed as co-catalysts to enhance the photo-catalytic degradation capabilities of composites [142]. Table 5 enlists various MXene-based catalysts for the successful photo-catalytic degradation of antibiotics.

The MXene-based photo-catalysts are also employed in literature for efficient environmental photo-catalysis like the removal of a range of antibiotics and pharmaceuticals from an aqueous environment because of their fascinating characteristics such as adjustable band gap (0.92–1.75 eV), appreciable safety, hydrophilicity, high strength and structural stability, large surface area, non-toxicity,

**Table 3**  
Removal of various heavy metal ions by MXene-based adsorbents.

MXene-based adsorbents	Surface area (m <sup>2</sup> g <sup>-1</sup> )	Heavy metal ions	Adsorption conditions			Adsorption capacity (mg g <sup>-1</sup> )	Adsorption mechanism	Reference
			pH	Time (min)	Temp. (K)			
<b>MXene/PEI modified sodium alginate aerogel (MPA)</b>	16.31	Cr <sup>6+</sup>	2	180	318	550.30	Chemical coordination, covalent bonding, chelation, chemical interactions, electrostatic attraction, adsorption, and reduction	[115]
<b>2D-Ti<sub>3</sub>C<sub>2</sub>T<sub>x</sub> MXenes</b>	11.2	Cr <sup>6+</sup>	3	40	30 ± 2 °C	104	Chemisorption, electrostatic attraction, complexation, surface interaction, particle diffusion, and ion exchange	[116]
<b>Sodium alginate/MXene/CoFe<sub>2</sub>O<sub>4</sub> (SA/MX/CFO) beads with rotating magnetic field (RMF)</b>	10.51	Cu <sup>2+</sup>	5.5	–	298	88.9	Magnetic and electrostatic interactions	[15]
<b>SA/MX/CFO beads without RMF</b>						104.1		
<b>MXene core (Ti<sub>3</sub>C<sub>2</sub>T<sub>x</sub>) shell aerogel spheres (MX-SA)</b>	9.66	Hg <sup>2+</sup>	4.5	24 h	298	932.84	Complex formation, ion-exchange, and electrostatic interactions	[117]
<b>2D alk-MXene (Ti<sub>3</sub>C<sub>2</sub>(OH/ONa)<sub>x</sub>F<sub>2-x</sub>)</b>	–	Pb <sup>2+</sup>	5.8	2	298	140	Electrostatic interactions, diffusion, and ion-exchange	[118]
<b>Ti<sub>3</sub>C<sub>2</sub>T<sub>x</sub> powder modified with silane coupling agent KH570 (Ti<sub>3</sub>C<sub>2</sub>T<sub>x</sub>-KH570)</b>	75.4	Pb <sup>2+</sup>	1–6	2 h	305	152.6	Ion-exchange, chelation, and chemisorption	[119]
<b>2D Ti<sub>3</sub>C<sub>2</sub>T<sub>x</sub> nanosheet</b>	13	Ba <sup>2+</sup>	7	2 h	298	9.3	Chemisorption and ion-exchange	[112]
<b>Alkalinized MXene/layered double metal hydroxide (alk-MXene/LDH)</b>	–	Ni <sup>2+</sup>	7	120	25 °C	222.7171	Ion exchange, surface complexation, chemisorption, physical adsorption, and chemical coordination	[120]

**Table 4**  
Removal of various antibiotics by MXene-based adsorbents.

MXene-based adsorbents	Surface area (m <sup>2</sup> g <sup>-1</sup> )	Antibiotics	Adsorption conditions			Adsorption capacity (mg g <sup>-1</sup> )	Adsorption mechanism	Reference
			pH	Time (min)	Temp. (K)			
Sodium Intercalated (SI) Ti <sub>3</sub> C <sub>2</sub> T <sub>x</sub> MXene	4.643	Ciprofloxacin	6	15–20	25 °C	208.2	Chemisorption and electrostatic interactions	[114]
Sodium ligninsulfonate functionalized MXene (Ti <sub>3</sub> C <sub>2</sub> -SL)	–	Doxorubicin hydrochloride (DOX)	7	180	30 °C	190.78	Physical adsorption, chemical adsorption, and intraparticle diffusion	[121]
Alkalized (ALK)-MXene	–	Tetracycline	5.5	10	40 °C	6.81 and ~57.85 with Ni <sup>2+</sup>	Surface complexation, electrostatic interactions, and chemisorption,	[122]
MXene (MX)-TiO <sub>2</sub>	–	Enrofloxacin (ENR)	–	–	–	1–6	Cation exchange and external adsorption	[123]
MXenes: Mn <sub>2</sub> C	–	Amoxicillin	–	–	–	–	Intermolecular interactions and H-bondings	[124]
		Ampicillin				–		
		Cloxacillin				55%		
Ti <sub>2</sub> C		Amoxicillin				88%		
		Ampicillin				44%		
		Cloxacillin				100%		
V <sub>2</sub> C		Amoxicillin				–		
		Ampicillin				–		
		Cloxacillin				66%		

high conductivity, environmental flexibility, and huge interlayer spacing [143–145]. MXenes are distinguished by their lamellar nanostructures with high conductivity and these materials have the potential to improve the photo-catalytic potential of their composites when employed as co-catalysts [146,147].

Generally, antibiotics in very low concentration have been perceived globally in a land environment and natural water; and are used by humans and other industries such as aquaculture, cattle, and poultry, thus can easily contaminate the environment [123,148]. These could enter the environment via different pathways such as domestic wastewater, industrial effluents and other waste streams, and livestock wastewater [149]. Their continuous disposal eventually leads to their gradual accumulation in an aquatic environment and the soil, from where they can also pass into the food chain.

MXenes have unveiled remarkable potential as co-catalysts for the photo-catalytic degradation of numerous pharmaceuticals because of their exceptional characteristics such as adjustable bandgap, activated metallic hydroxide sites, availability of numerous surface functional groups, biocompatibility, hydrophilicity, high specific surface area, high metallic conductivity, ease of functionalization, and fast photo-generated charge carrier separation ability [75,140]. A recent study assessed the confiscation of enrofloxacin antibiotic compounds from water by the use of newly developed multi-functional adsorbent photo-catalyst MXene-TiO<sub>2</sub> composites by hydrothermal treatment [123]. In addition to this, the layered MXene structure can also enhance the photo-catalytic activity by promoting the photo-generated charge carrier separation, limiting the size of photo-catalysts, enhancing reacting adsorption, and acting as a robust support [140].

The MXenes materials exhibited exceptional potential in the photo-catalytic degradation of various antibiotics and pharmaceutical compounds. MXenes can be also used as a host material to enhance the catalytic performance of different co-catalysts. Numerous methods have been employed for the development of MXene-based photo-catalysts for successful degradation of pharmaceuticals such as anodization, chemical vapor deposition, in-situ growth method, sol-hydrothermal method, evaporation-induced self-assembly method, in-situ reductive deposition method [75].

In the case of NH<sub>2</sub>-MIL-125(Ti)(TiO<sub>2</sub>)/Ti<sub>3</sub>C<sub>2</sub> for the efficient degradation of TC-HCl, the better photo-catalytic performance of the hetero-junction is ascribed to the enhanced characteristics after the Ti<sub>3</sub>C<sub>2</sub> incorporation, which improved the charge transfer [150]. The pharmaceutical (TC-HCl) degradation includes the 'OH' formation by water oxidation and electrons activation from the valence band (VB) to the conduction band (CB) for the employed NH<sub>2</sub>-MIL-125(Ti). Similarly, the electron migration from the NH<sub>2</sub>-MIL-125 (Ti) CB to the TiO<sub>2</sub> CB; and then from TiO<sub>2</sub> to Ti<sub>3</sub>C<sub>2</sub> transpires through the hetero-junction. The formation of the Schottky junction performs as an electron trap to catch the photo-induced electrons that are transferred to the Ti<sub>3</sub>C<sub>2</sub> surface for electron-oxygen reduction.

In the case of the photo-catalytic degradation of carbamazepine by the hetero-structural TiO<sub>2</sub>/Ti<sub>3</sub>C<sub>2</sub>T<sub>x</sub> (MXene), the generated electrons at the surface of the TiO<sub>2</sub> are prohibited from being shifted to Ti<sub>3</sub>C<sub>2</sub>T<sub>x</sub> sheets at the interface (Fig. 7a) [151]. Such barred transferring is ascribed to the following reasons: (i) MXene's work function is much lower compared to TiO<sub>2</sub>, and (ii) MXene has a higher negative Fermi level compared to the TiO<sub>2</sub> CB [151].

Another study reported the use of a novel CuFe<sub>2</sub>O<sub>4</sub>/MXene (CFO/Ti<sub>3</sub>C<sub>2</sub>) hetero-junction photo-catalyst that unveiled substantial synergic visible light degradation of sulfamethazine (SMZ), which is ascribed to the enhanced lifetime of carriers and photo-electrons transfer in the employed composite [141]. Fig. 7b illustrates the mechanism of the photocatalytic degradation of the SMZ by the employed CFO/Ti<sub>3</sub>C<sub>2</sub> photo-catalyst, under visible light. The CuFe<sub>2</sub>O<sub>4</sub> (CFO), with a band gap of 1.43 eV, is excited by the visible light, and the photo-generated electrons are excited from the VB to CB. In the case of CFO/Ti<sub>3</sub>C<sub>2</sub>, the photo-induced electrons are shifted to the 2D Ti<sub>3</sub>C<sub>2</sub> from the CFO; while, numerous electrons appear near the Fermi level in the Ti<sub>3</sub>C<sub>2</sub> flakes, making it somehow metallic in

**Table 5**  
Photocatalytic degradation of antibiotics by MXene-based catalysts.

MXene-based catalysts	Specific surface area ( $\text{m}^2 \text{g}^{-1}$ )	Pollutants	Degradation conditions				Degradation (%)	Reactive species	Light source	Reference
			pH	Catalyst dosage (mg)	Time (min)	Temp. (K)				
CdS@Ti <sub>3</sub> C <sub>2</sub> @TiO <sub>2</sub>	42.38	Sulfachloropyridazine	–	50	88	25 °C	~100	•O <sub>2</sub> <sup>-</sup> and •OH	Visible light (300 mW cm <sup>-2</sup> )	[152]
Few-layer MXene/alkaline g-C <sub>3</sub> N <sub>4</sub>	37.2	Tetracycline (TC-HCl)	–	10	60	–	77	h <sup>+</sup> , •OH, •O <sub>2</sub> <sup>-</sup> , and e <sup>-</sup>	Visible light (>420 nm)	[153]
Magnetic Ti <sub>3</sub> C <sub>2</sub> T <sub>x</sub>	118.022	Diclofenac	5–9	3 g/L	30	293	~100	HO•, Cl•, O <sub>2</sub> <sup>•-</sup> , h <sup>+</sup> , and e <sup>-</sup>	UV (1.35 ±0.2 mW cm <sup>-2</sup> )	[154]
MXene-Ti <sub>3</sub> C <sub>2</sub> /MoS <sub>2</sub>	11.93	Ranitidine	–	5	60	–	88.4	•O <sub>2</sub> <sup>-</sup> , h <sup>+</sup> , and •OH	LED lamp (25 W, Trusttech PLS-SXE 300)	[155]
Ti <sub>3</sub> C <sub>2</sub> /TiO <sub>2</sub> /BiOCl	8.774	TC	–	50	120	–	~100	•O <sub>2</sub> <sup>-</sup> and •OH	500 W Xe lamp	[156]
Ti <sub>3</sub> C <sub>2</sub> /g-C <sub>3</sub> N <sub>4</sub>	–	Levofloxacin	–	20	30	Room	72	–	300 W Xe lamp	[157]
Oxygen-vacancy-embedded 2D/2D NiFe-LDH/Ti <sub>3</sub> C <sub>2</sub> T <sub>x</sub> MXene composite	–	Norfloxacin	–	20 mg/50 mL	240	–	98	•O <sub>2</sub> <sup>-</sup> , •OH, and h <sup>+</sup>	300 W Xe lamp	[158]



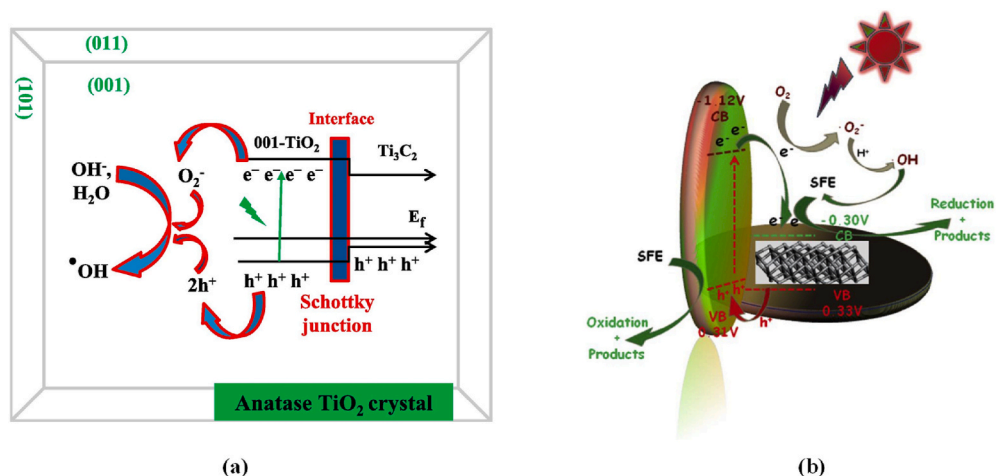


**Fig. 7.** (a) Schematic illustration of the degradation mechanism of CBZ by the 001-T/MX photo-catalyst. Reprinted with permission from Ref. [151]. Copyright (2018), Elsevier B.V., (b) Possible degradation mechanism of CFO/Ti<sub>3</sub>C<sub>2</sub> for degrading SMZ. Reprinted with permission from Ref. [141]. Copyright (2020), Elsevier B.V.

nature (trapping location for light-induced electrons) [141]. Moreover, Ti<sub>3</sub>C<sub>2</sub> can also provide numerous active adsorption sites due to its large specific surface area. Besides, the antibiotic molecules (SMZ) could also be adsorbed by the active material throughout the photo-catalysis process. Fig. 8 shows the SMZ degradation into the low-molecular-weight organic compounds (aminobenzenes and methylpyrimidines) [151].

These studies reflect the importance of MXene-based photo-catalysts for the successful photo-catalytic degradation of numerous antibiotics and pharmaceuticals in the next-generation photo-catalysis.

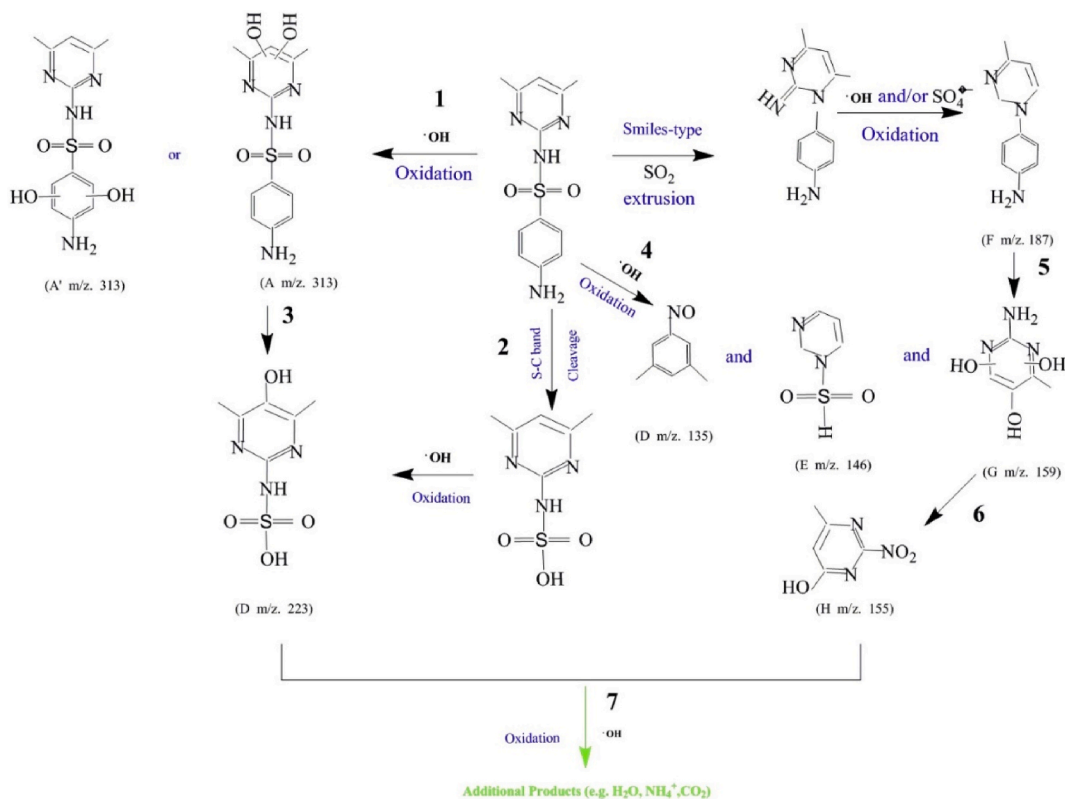


**Fig. 8.** Analysis of degradation intermediates and possible degradation pathways of SMZ. Reprinted with permission from Ref. [151]. Copyright (2020), Elsevier B.V.

#### 4. Comparison of MXene-based membranes with other 2D materials

MXenes are a new class of 2D materials, along with 2D zeolites, MOFs, COFs, graphitic carbon nitride (g-C<sub>3</sub>N<sub>4</sub>), graphene, graphene oxide (GO), and layered TMDCs [60,159–162]. There is a promising future for molecular separation applications using most of these 2D materials [163,164]. Two broad categories of 2D material-based membranes are spongy nanosheet membranes and laminar membranes (Fig. 9) [159]. Additionally, 2D materials can be employed as a filler to offset the characteristics of the polymeric membranes, as shown in Fig. 10a [165]. The separation efficiency of 2D membranes depends on their physicochemical properties and molecular transport pathway. The transport pathways of 2D materials can be manipulated to achieve a precise molecular separation. Nanochannels can form horizontal or vertical pathways in laminar membranes (Fig. 10b and c) [165].

The frequently employed assembly for the non-porous nanosheets, such as MXenes and GO, are the laminar membranes. Although laminar membrane structure is expected to have less permeation rates compared to porous membranes such as porous graphene, MOFs, and zeolite nanosheets; however, their facile synthesis methods still make them potential candidates for large-scale applications [159].

Although a direct comparison of MXenes with other 2D materials is impractical because the performance of membranes can better be judged under similar conditions. However, this section aims to overview the efficiency of numerous 2D materials for the separation of specific pollutants including antibiotics and heavy metals.

A comparative analysis of MXene-based membranes with membranes prepared from other 2D materials for the removal of selected pollutants is presented in Table 6. The efficiency of MXene-based membranes is comparable to or better than most of the 2D membranes, offering in special cases separation efficiency as high as 99% and compelling productivities in terms of permeate flux. This demonstrates the significance of using these membranes for water purification in the near future.

#### 5. Conclusions, challenges, and future perspective

This review covers a research gap dealing with the elucidation of the latest advances in MXenes membranes and materials (adsorbents and photo-catalysts) for selective separations in water treatments, including the removal of heavy metals and antibiotics. These pollutants represent a serious environmental concern since they affect the quality of water bodies, thus severely affecting living organisms. Here, it has been proved the outperforming separation of MXenes membranes and materials for the removal of such toxic compounds. Moreover, MXene-based composites have drawn lots of interest as photo-catalysts to degrade contaminants because of their outstanding thermal and optical characteristics, hydrophilicity, significant surface area, configurable chemical characteristics, high chemical stability, regular planar configurations, high metallic conductivity, and so many derivative products. It was found that literature reported numerous MXene-based membranes with fascinating separation performance compared to other available 2D materials. MXene-based membranes have shown remarkable potential in water treatment, but still there exist many challenges that need careful attention because these hurdles prevent them from their actual applications in the real water environment. Some of the key challenges and recommendations are summarized below.

- The HF-synthesis methods for the mass production of MXenes should be minimized because of their drastic ecological concerns and therefore other innovative and sustainable alternative green synthesis techniques should be adopted.
- MXenes are currently produced on lab-scale costly processes but with lower yields. Therefore, MXene synthesis via commercial routes should be at the forefront of present-day researchers to develop cheap, efficient, and environmentally friendly MXenes.
- The application of MXene-based membranes in the actual environment (real water system) should be explored since it is almost missing in the literature. Therefore, these membranes should be at the forefront of future studies in order to challenge their efficacy in the actual water environment.
- The mechanisms of pollutants from wastewater should be explored in much detail and an in-depth analysis should be carried out by using different available characterization tools and theoretical models.
- A particular focus should be placed on the regeneration of the membranes employed and the successful removal of pollutants retained on their surfaces. This would achieve long-term membrane stability by keeping its cost much lower and the membrane much more beneficial.
- One of the key challenges is the storage and stability of MXene because of its oxidizing nature in the water environment. Therefore, the future research area should cope with this trial by exploring different pathways for its mitigations. This will help in developing the MXene's stability and its wide range of applications.
- Various theoretical and experimental methods should be adopted for optimum water fluxes through the studied membranes since these can be directly controlled by the flake sizes of the employed MXenes.
- The stability of MXene nanosheets is a critical parameter in assessing its potential since it directly affects the overall lifespan of these materials. Therefore, future research in this direction might lead to more stable MXene structures that in turn would be employed in treating a wide range of hazardous pollutants from actual wastewater streams.
- The applications of MXene-based membranes in removing simultaneous pollutants from an aqueous environment should be explored because real wastewater streams are comprised of different kinds of contaminants and pollutants.
- The elimination of various pollutants by photo-catalysis via the employment of MXenes should also be explored because extra efforts are needed to develop well-connected interfaces to enhance photon adsorption and charge-carrier transportation [173]. This in turn would cause superior redox capability and enhanced interfacial arrangements which could develop efficient photocatalysts with robust degradation abilities.

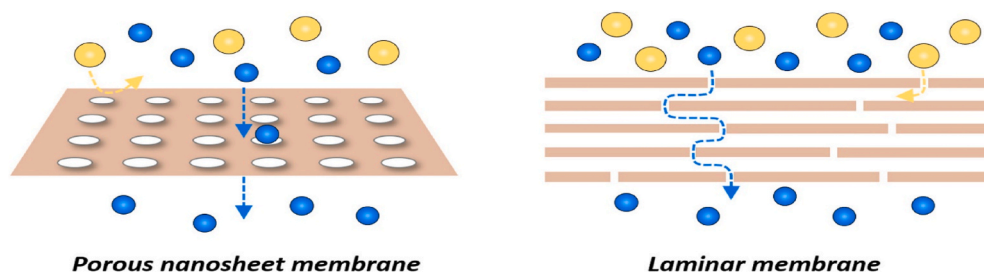


**Fig. 9.** Schematic of two types of 2D materials membranes: porous nanosheet membranes and lamellar membranes. Reprinted with permission from Ref. [159]. Copyright (2021), American Chemical Society.

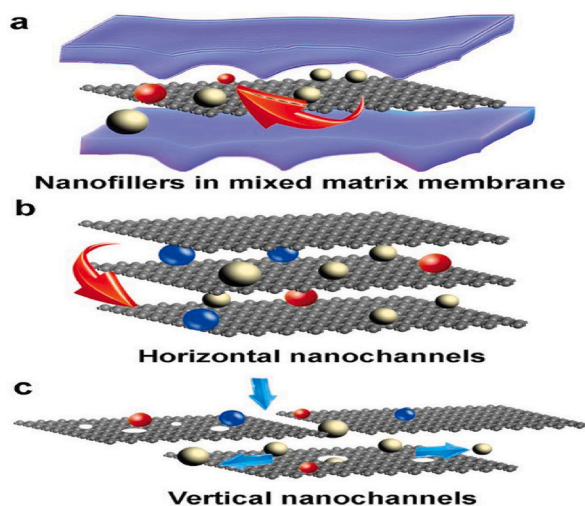


**Fig. 10.** Schematic illustrations of the separation mechanism of 2D material membranes. Reprinted with permission from Ref. [165]. Copyright (2020), Wiley-VCH GmbH.

**Table 6**

Comparison of the performance of MXene-based membranes with other 2D materials.

Membrane	Pollutant	Concentration (mg/L)	Water permeability (L m <sup>-2</sup> h <sup>-1</sup> bar <sup>-1</sup> )	Separation/rejection efficiency (%)	Reference
SWCNT-intercalated GO ultrathin films	Cytochrome c	125	700 ± 50	98.3 ± 0.2	[166]
2D Ti <sub>3</sub> C <sub>2</sub> T <sub>x</sub> MXene nanosheets	Cytochrome c	20	1056 ± 25	97 ± 1	[167]
Lamellar graphene oxide (LGO)	Evans blue (EB)	–	71	85	[168]
Laminar MoS <sub>2</sub>	EB	15 μM	245	89	[169]
Layered WS <sub>2</sub> membranes	EB	15 μM	450	90	[170]
2D Ti <sub>3</sub> C <sub>2</sub> T <sub>x</sub> MXene nanosheets	EB	10	1084 ± 47	90 ± 1	[167]
TFN membrane with GO	Zn <sup>2+</sup>	50–1000	18.03	93.33	[171]
	Cu <sup>2+</sup>			92.73	
	Ni <sup>2+</sup>			90.45	
	Pb <sup>2+</sup>			88.35	
Thermal cross-linked 2D MXene (Ti <sub>2</sub> C <sub>3</sub> T <sub>x</sub> ) membrane	Pb <sup>2+</sup>	~100	~250 L m <sup>-2</sup> h <sup>-1</sup>	Hydrated rejection of Pb <sup>2+</sup> : 99	[89]
PFDTMS-modified hydrophobic 2D d-Ti <sub>3</sub> C <sub>2</sub> membrane	Cu <sup>2+</sup>	–	–	~100	[78]
Polythiocyanuric acid-functionalized MoS <sub>2</sub> nanosheet-based high flux membranes	Hg <sup>2+</sup>	10	246 L m <sup>-2</sup> h <sup>-1</sup>	80	[172]
	Cr <sup>6+</sup>				
	Pb <sup>2+</sup>				
MXene-anchored goethite heterogeneous Fenton composite (β-FeOOH@MXene <sub>0.2</sub> ) freestanding membrane	Hg <sup>2+</sup>	60	–	99.7	[79]

- Various theoretical calculations such as the density functional theory and first principles methods should be explored and introduced into the design of the MXene-based photo-catalysts in order to envisage the future structural performance and understand the photo-catalytic mechanism at the micro-level and the overall photo-catalytic process [145].
- Critical and widespread research is needed in the development and applications of MXene-based membranes for identifying crosslinkers and substrates for the membrane influencing its performance [174].

#### Author contribution statement

FAJ: Conceptualization, Writing- Original draft preparation, RCM: Reviewing, Methodology. II: Visualization, Investigation. MB: Writing, Investigation, FG: Reviewing and Editing, GB: Supervision, Editing.

#### Declaration of competing interest

The authors declare that they have no known competing financial interests or personal relationships that could have appeared to influence the work reported in this paper.

#### Data availability

Data will be made available on request.

#### Acknowledgements

Financial support from Nobelium Joining Gdańsk Tech Research Community (contract number DEC 33/2022/IDUB/1.1; NOBELIUM nr 036236) is gratefully acknowledged. R. Castro-Muñoz also acknowledges the School of Engineering and Science and the FEMSA-Biotechnology Center at Tecnológico de Monterrey for their support through the Bioprocess (0020209113) Focus Group.

#### References

- [1] J.K. Im, E.J. Sohn, S. Kim, M. Jang, A. Son, K.D. Zoh, Y. Yoon, Review of MXene-based nanocomposites for photocatalysis, *Chemosphere* 270 (2021), 129478, <https://doi.org/10.1016/j.chemosphere.2020.129478>.
- [2] A. Bhatnagar, M. Sillanpää, A. Witek-Krowiak, Agricultural waste peels as versatile biomass for water purification—A review, *Chem. Eng. J.* 270 (2015) 244–271.
- [3] S. Lustenberger, R. Castro-Muñoz, Advanced biomaterials and alternatives tailored as membranes for water treatment and the latest innovative European water remediation projects: a review, *Case Stud. Chem. Environ. Eng.* 5 (2022), <https://doi.org/10.1016/j.csee.2022.100205>.
- [4] A. Azimi, A. Azari, M. Rezakazemi, M. Ansarpour, Removal of heavy metals from industrial wastewaters: a review, *ChemBioEng Rev* 4 (2017) 37–59, <https://doi.org/10.1002/cben.201600010>.
- [5] F. Fu, Q. Wang, Removal of heavy metal ions from wastewaters: a review, *J. Environ. Manag.* 92 (2011) 407–418, <https://doi.org/10.1016/j.jenvman.2010.11.011>.
- [6] C. Ursino, R. Castro-Muñoz, E. Drioli, L. Gzara, M.H. Albeirutty, A. Figoli, Progress of nanocomposite membranes for water treatment, *Membranes* 8 (2018), <https://doi.org/10.3390/membranes8020018>.
- [7] M.E. Valdés, L.H. Santos, M.C.R. Castro, A. Giorgi, D. Barceló, S. Rodríguez-Mozaz, M.V. Amé, Distribution of antibiotics in water, sediments and biofilm in an urban river (Córdoba, Argentina, LA), *Environ. Pollut.* 269 (2021), 116133.
- [8] X. Yang, Y. Liu, S. Hu, F. Yu, Z. He, G. Zeng, Z. Feng, A. Sengupta, Construction of Fe<sub>3</sub>O<sub>4</sub>@ MXene composite nanofiltration membrane for heavy metal ions removal from wastewater, *Polym. Adv. Technol.* 32 (2021) 1000–1010, <https://doi.org/10.1002/pat.5148>.
- [9] A. Abbas Ihsanullah, A.M. Al-Amer, T. Laoui, M.J. Al-Marri, M.S. Nasser, M. Khraisheh, M.A. Atieh, Heavy metal removal from aqueous solution by advanced carbon nanotubes: critical review of adsorption applications, *Separ. Purif. Technol.* 157 (2016) 141–161, <https://doi.org/10.1016/j.seppur.2015.11.039>.
- [10] R. Castro-Muñoz, E. Gontarek, A. Figoli, Membranes for Toxic- and Heavy-Metal Removal, 2019, <https://doi.org/10.1016/B978-0-12-816778-6.00007-2>.
- [11] R. Castro-Muñoz, B.E. Barragán-Huerta, V. Ffla, P.C. Denis, R. Ruby-Figueroa, Current Role of Membrane Technology: from the Treatment of Agro-Industrial By-Products up to the Valorization of Valuable Compounds, Waste and Biomass Valorization, 2017, <https://doi.org/10.1007/s12649-017-0003-1>.
- [12] M. Bilal, I. Ihsanullah, M. Younas, M. Ul Hassan Shah, Recent advances in applications of low-cost adsorbents for the removal of heavy metals from water: a critical review, *Separ. Purif. Technol.* 278 (2022), 119510, <https://doi.org/10.1016/j.seppur.2021.119510>.
- [13] D. Mangla, A. Sharma, S. Ikram, Critical review on adsorptive removal of antibiotics: present situation, challenges and future perspective, *J. Hazard Mater.* 425 (2022), 127946.
- [14] G.G. Hacrosmanoğlu, C. Mejías, J. Martín, J.L. Santos, I. Aparicio, E. Alonso, Antibiotic adsorption by natural and modified clay minerals as designer adsorbents for wastewater treatment: a comprehensive review, *J. Environ. Manag.* 317 (2022), 115397.
- [15] J. Ren, Z. Zhu, Y. Qiu, F. Yu, T. Zhou, J. Ma, J. Zhao, Enhanced adsorption performance of alginate/MXene/CoFe<sub>2</sub>O<sub>4</sub> for antibiotic and heavy metal under rotating magnetic field, *Chemosphere* 284 (2021), 131284, <https://doi.org/10.1016/j.chemosphere.2021.131284>.
- [16] R. Chakraborty, A. Asthana, A.K. Singh, B. Jain, A.B.H. Susan, Adsorption of heavy metal ions by various low-cost adsorbents: a review, *Int. J. Environ. Anal. Chem.* 102 (2022) 342–379, <https://doi.org/10.1080/03067319.2020.1722811>.
- [17] M.A. Shaida, R.K. Dutta, A.K. Sen, S.S. Ram, M. Sudarshan, M. Naushad, G. Boczkaj, M.S. Nawab, Chemical analysis of low carbon content coals and their applications as dye adsorbent, *Chemosphere* 287 (2022), 132286, <https://doi.org/10.1016/j.chemosphere.2021.132286>.
- [18] B. Kakavandi, A. Raofi, S.M. Peyghambarzadeh, B. Ramavandi, M.H. Niri, M.%J.D. Ahmadi, W. Treatment, Efficient adsorption of cobalt on chemical modified activated carbon: characterization, optimization and modeling studies 111 (2018) 310–321.
- [19] Y. Zhang, Y.-G. Zhao, F. Maqbool, Y. Hu, Removal of antibiotics pollutants in wastewater by UV-based advanced oxidation processes: influence of water matrix components, processes optimization and application: a review, *J. Water Proc. Eng.* 45 (2022), 102496.
- [20] J. Du, B. Zhang, J. Li, B. Lai, Decontamination of heavy metal complexes by advanced oxidation processes: a review, *Chin. Chem. Lett.* 31 (2020) 2575–2582, <https://doi.org/10.1016/J.CCLET.2020.07.050>.
- [21] E. Cako, Z. Wang, R. Castro-Muñoz, M.P. Rayaroth, G. Boczkaj, Cavitation based cleaner technologies for biodiesel production and processing of hydrocarbon streams: a perspective on key fundamentals, missing process data and economic feasibility – a review, *Ultrason. Sonochem.* 88 (2022), <https://doi.org/10.1016/j.ultrasonch.2022.106081>.

- [22] D. Lin, Y. Fu, X. Li, L. Wang, M. Hou, D. Hu, Q. Li, Z. Zhang, C. Xu, S. Qiu, Z. Wang, G. Boczkaj, Application of persulfate-based oxidation processes to address diverse sustainability challenges: a critical review, *J. Hazard Mater.* 440 (2022), 129722, <https://doi.org/10.1016/j.jhazmat.2022.129722>.
- [23] N. Nasrollahi, V. Vatanpour, A. Khataee, Removal of antibiotics from wastewaters by membrane technology: limitations, successes, and future improvements, *Sci. Total Environ.* (2022), 156010.
- [24] J. Zheng, Y. Li, D. Xu, R. Zhao, Y. Liu, G. Li, Q. Gao, X. Zhang, A. Volodine, B. Van der Bruggen, Facile fabrication of a positively charged nanofiltration membrane for heavy metal and dye removal, *Separ. Purif. Technol.* 282 (2022), 120155, <https://doi.org/10.1016/J.SEPUR.2021.120155>.
- [25] F. Ahmed Janjhi, I. Chandio, A. Ali Memon, Z. Ahmed, K. Hussain Thebo, A. Ali Ayaz Pirzado, A. Ali Hakro, M. Iqbal, Functionalized graphene oxide based membranes for ultrafast molecular separation, *Separ. Purif. Technol.* 274 (2021), 117969, <https://doi.org/10.1016/j.seppur.2020.117969>.
- [26] K.H. Thebo, X. Qian, Q. Zhang, L. Chen, H.-M. Cheng, W. Ren, Highly stable graphene-oxide-based membranes with superior permeability, *Nat. Commun.* 9 (2018) 1486, <https://doi.org/10.1038/s41467-018-03919-0>.
- [27] R. Castro-Muñoz, Retention profile on the physicochemical properties of maize cooking by-product using a tight ultrafiltration membrane, *Chem. Eng. Commun.* (2019) 1–9, <https://doi.org/10.1080/00986445.2019.1618844>.
- [28] R. Castro-Muñoz, K.V. Agrawal, Z. Lai, J. Coronas, Towards large-scale application of nanoporous materials in membranes for separation of energy-relevant gas mixtures, *Separ. Purif. Technol.* 308 (2023), 122919.
- [29] N. Ottman, L. Ruokolainen, A. Suomalainen, H. Sinkko, P. Karisola, J. Lehtimäki, M. Lehto, I. Hanski, H. Alenius, N. Fyhrquist, Soil exposure modifies the gut microbiota and supports immune tolerance in a mouse model, *J. Allergy Clin. Immunol.* 143 (2019) 1198–1206. e12.
- [30] A. Fernandes, P. Makoś, Z. Wang, G. Boczkaj, Synergistic effect of TiO<sub>2</sub> photocatalytic advanced oxidation processes in the treatment of refinery effluents, *Chem. Eng. J.* 391 (2020), 123488, <https://doi.org/10.1016/j.cej.2019.123488>.
- [31] A. Dąbrowski, Z. Hubicki, P. Podkościelny, E. Robens, Selective removal of the heavy metal ions from waters and industrial wastewaters by ion-exchange method, *Chemosphere* 56 (2004) 91–106, <https://doi.org/10.1016/j.chemosphere.2004.03.006>.
- [32] M.C. Benalia, L. Youcef, M.G. Bouaziz, S. Achour, H. Menasra, Removal of heavy metals from industrial wastewater by chemical precipitation: mechanisms and sludge characterization, *Arabian J. Sci. Eng.* 47 (2022) 5587–5599, <https://doi.org/10.1007/s13369-021-05525-7>.
- [33] J.-M. Arana Juve, F. Munk Christensen, Y. Wang, Z. Wei, Electrodialysis for metal removal and recovery: a review, *Chem. Eng. J.* 435 (2022), 134857, <https://doi.org/10.1016/j.cej.2022.134857>.
- [34] A. Shoneye, J. Sen Chang, M.N. Chong, J. Tang, Recent progress in photocatalytic degradation of chlorinated phenols and reduction of heavy metal ions in water by TiO<sub>2</sub>-based catalysts, *Int. Mater. Rev.* 67 (2022) 47–64, <https://doi.org/10.1080/09506608.2021.1891368>.
- [35] A. Fernandes, M. Gagol, P. Makoś, J.A. Khan, G. Boczkaj, Integrated photocatalytic advanced oxidation system (TiO<sub>2</sub>/UV/O<sub>3</sub>/H<sub>2</sub>O<sub>2</sub>) for degradation of volatile organic compounds, *Separ. Purif. Technol.* 224 (2019) 1–14, <https://doi.org/10.1016/j.seppur.2019.05.012>.
- [36] V.K. Landge, S.H. Sonawane, M. Sivakumar, S.S. Sonawane, G. Uday Bhaskar Babu, G. Boczkaj, S-scheme heterojunction Bi<sub>2</sub>O<sub>3</sub>-ZnO/Bentonite clay composite with enhanced photocatalytic performance, *Sustain. Energy Technol. Assessments* 45 (2021), 101194, <https://doi.org/10.1016/j.seta.2021.101194>.
- [37] F. Hasanvandian, A. Shokri, M. Moradi, B. Kakavandi, S. Rahman Setayesh, Encapsulation of spinel CuCo<sub>2</sub>O<sub>4</sub> hollow sphere in V<sub>2</sub>O<sub>5</sub>-decorated graphitic carbon nitride as high-efficiency double Z-type nanocomposite for levofloxacin photodegradation, *J. Hazard Mater.* 423 (2022), 127090, <https://doi.org/10.1016/j.jhazmat.2021.127090>.
- [38] F. Hasanvandian, M. Moradi, S. Aghaebrahimi Samani, B. Kakavandi, S. Rahman Setayesh, M. Noorisepehr, Effective promotion of g-C<sub>3</sub>N<sub>4</sub> photocatalytic performance via surface oxygen vacancy and coupling with bismuth-based semiconductors towards antibiotics degradation, *Chemosphere* 287 (2022), 132273, <https://doi.org/10.1016/j.chemosphere.2021.132273>.
- [39] S.T. Malkapuram, V. Sharma, S.P. Gumfekar, S. Sonawane, S. Sonawane, G. Boczkaj, M.M. Seepana, A review on recent advances in the application of biosurfactants in wastewater treatment, *Sustain. Energy Technol. Assessments* 48 (2021), 101576, <https://doi.org/10.1016/j.seta.2021.101576>.
- [40] M. Shen, Y. Zhang, E. Almatrafi, T. Hu, C. Zhou, B. Song, Z. Zeng, G. Zeng, Efficient removal of microplastics from wastewater by an electrocoagulation process, *Chem. Eng. J.* 428 (2022), 131161.
- [41] R. Ahmed, A.K. Hamid, S.A. Krebsbach, J. He, D. Wang, Critical review of microplastics removal from the environment, *Chemosphere* (2022), 133557.
- [42] M.S. de Ilurdoz, J.J. Sadhwani, J.V. Reboso, Antibiotic removal processes from water & wastewater for the protection of the aquatic environment—a review, *J. Water Proc. Eng.* 45 (2022), 102474.
- [43] S.A. Razzak, M.O. Faruque, Z. Alsheikh, L. Alsheikhmohamad, D. Alkuroud, A. Alfayez, S.M.Z. Hossain, M.M. Hossain, A comprehensive review on conventional and biological-driven heavy metals removal from industrial wastewater, *Environ. Adv.* 7 (2022), 100168, <https://doi.org/10.1016/J.ENVADV.2022.100168>.
- [44] P. Fatehbasharzad, S. Aliasghari, I. Shaterzadeh Tabrizi, J.A. Khan, G. Boczkaj, Microbial fuel cell applications for removal of petroleum hydrocarbon pollutants: a review, *Water Resour. Int.* 28 (2022), 100178, <https://doi.org/10.1016/j.wri.2022.100178>.
- [45] M. Khatami, S. Irvani, M. Khatami, Comments on inorganic chemistry A journal of critical discussion of the current literature MXenes and MXene-based materials for the removal of water pollutants: challenges and opportunities MXenes and MXene-based materials for the removal of water pollut, *Comments Mod. Chem.* 41 (2021) 213–248, <https://doi.org/10.1080/02603594.2021.1922396>.
- [46] S. Moradi, A.A. Isari, F. Hayati, R. Rezaei Kalantary, B. Kakavandi, Co-implanting of TiO<sub>2</sub> and liquid-phase-delaminated g-C<sub>3</sub>N<sub>4</sub> on multi-functional graphene nanobridges for enhancing photocatalytic degradation of acetaminophen, *Chem. Eng. J.* 414 (2021), 128618, <https://doi.org/10.1016/j.cej.2021.128618>.
- [47] X. Li, J. Yu, J. Low, Y. Fang, J. Xiao, X. Chen, Engineering heterogeneous semiconductors for solar water splitting, *J. Mater. Chem. A.* 3 (2015) 2485–2534, <https://doi.org/10.1039/C4TA004461D>.
- [48] F. Hasanvandian, M. Zehtab Salmasi, M. Moradi, S. Farshineh Saei, B. Kakavandi, S. Rahman Setayesh, Enhanced spatially coupling heterojunction assembled from CuCo<sub>2</sub>S<sub>4</sub> yolk-shell hollow sphere encapsulated by Bi-modified TiO<sub>2</sub> for highly efficient CO<sub>2</sub> photoreduction, *Chem. Eng. J.* 444 (2022), 136493, <https://doi.org/10.1016/j.cej.2022.136493>.
- [49] Y. Ren, D. Zeng, W.-J. Ong, Interfacial engineering of graphitic carbon nitride (g-C<sub>3</sub>N<sub>4</sub>)-based metal sulfide heterojunction photocatalysts for energy conversion: a review, *Chin. J. Catal.* 40 (2019) 289–319, [https://doi.org/10.1016/S1872-2067\(19\)63293-6](https://doi.org/10.1016/S1872-2067(19)63293-6).
- [50] S. Wang, B.Y. Guan, Y. Lu, X.W. David Lou, formation of hierarchical In<sub>2</sub>S<sub>3</sub>-CdIn<sub>2</sub>S<sub>4</sub> heterostructured nanotubes for efficient and stable visible light CO<sub>2</sub> reduction, *J. Am. Chem. Soc.* 139 (2017) 17305–17308, <https://doi.org/10.1021/jacs.7b10733>.
- [51] I. Ihsanullah, Applications of MOFs as adsorbents in water purification: progress, challenges and outlook, *Curr. Opin. Environ. Sci. Heal.* (2022), 100335, <https://doi.org/10.1016/j.coesh.2022.100335>.
- [52] R. Castro-Muñoz, Breakthroughs on tailoring pervaporation membranes for water desalination: a review, *Water Res.* 187 (2020), 116428, <https://doi.org/10.1016/j.watres.2020.116428>.
- [53] E. Gontarek-Castro, R. Castro-Muñoz, M. Lieder, New insights of nanomaterials usage toward superhydrophobic membranes for water desalination via membrane distillation: a review, *Crit. Rev. Environ. Sci. Technol.* (2021), <https://doi.org/10.1080/10643389.2021.1877032>.
- [54] E. Gontarek-Castro, M.K. Rybarczyk, R. Castro-Muñoz, M. Morales-Jiménez, B. Barragán-Huerta, M. Lieder, Characterization of PVDF/graphene nanocomposite membranes for water desalination with enhanced antifungal activity, *Water (Switzerland)* (2021) 13, <https://doi.org/10.3390/w13091279>.
- [55] R. Castro-Muñoz, A. Cruz-Cruz, Y. Alfaro-Sommers, L.X. Aranda-Jarillo, E. Gontarek-Castro, Reviewing the recent developments of using graphene-based nanosized materials in membrane separations, *Crit. Rev. Environ. Sci. Technol.* (2021) 1–38, <https://doi.org/10.1080/10643389.2021.1918509>.
- [56] R. Castro-Muñoz, J. Buera-González, O. de la Iglesia, F. Galiano, V. Fila, M. Malankowska, C. Rubio, A. Figoli, C. Téllez, J. Coronas, Towards the dehydration of ethanol using pervaporation cross-linked poly(vinyl alcohol)/graphene oxide membranes, *J. Membr. Sci.* 582 (2019) 423–434, <https://doi.org/10.1016/j.memsci.2019.03.076>.
- [57] R. Castro-muñoz, Progress on incorporating zeolites in matrimid® 5218 mixed matrix membranes towards gas separation, *Membranes* 8 (2018) 30, <https://doi.org/10.3390/membranes8020030>.
- [58] M.Z. Ahmad, V. Martin-Gil, T. Supinkova, P. Lambert, R. Castro-Muñoz, P. Hrabanek, M. Kocirik, V. Fila, Novel MMM using CO<sub>2</sub> selective SSZ-16 and high-performance 6FDA-polyimide for CO<sub>2</sub>/CH<sub>4</sub> separation, *Separ. Purif. Technol.* 254 (2021), 117582, <https://doi.org/10.1016/j.seppur.2020.117582>.



- [59] R. Castro-Muñoz, V. Fíla, V. Martín-Gil, C. Muller, Enhanced CO<sub>2</sub> permeability in Matrimid® 5218 mixed matrix membranes for separating binary CO<sub>2</sub>/CH<sub>4</sub> mixtures, *Sep. Purif. Technol.* 210 (2019) 553–562, <https://doi.org/10.1016/j.seppur.2018.08.046>.
- [60] P. Liu, J. Hou, Y. Zhang, L. Li, X. Lu, Z. Tang, Two-dimensional material membranes for critical separations, *Inorg. Chem. Front.* 7 (2020) 2560–2581, <https://doi.org/10.1039/d0qi00307g>.
- [61] R. Castro-Muñoz, F. Galiano, Ó. de la Iglesia, V. Fíla, C. Tellez, J. Coronas, A. Figoli, Graphene oxide – filled polyimide membranes in pervaporative separation of azeotropic methanol – MTBE mixtures, *Separ. Purif. Technol.* 224 (2019) 265–272, <https://doi.org/10.1016/j.seppur.2019.05.034>.
- [62] R. Castro-Muñoz, L.L. González-Melgoza, O. García-Depraect, Ongoing progress on novel nanocomposite membranes for the separation of heavy metals from contaminated water, *Chemosphere* 270 (2021), <https://doi.org/10.1016/j.chemosphere.2020.129421>.
- [63] M. Naguib, O. Mashtalir, J. Carle, V. Presser, J. Lu, L. Hultman, Y. Gogotsi, M.W. Barsoum, T.-D.T.M. Carbides, *ACS Nano* 6 (2012) 1322. Crossref, ISI. (n.d.).
- [64] R. Castro-Munoz, MXene : a two-dimensional material in selective water separation via pervaporation, *Arab. J. Chem.* 15 (2022), 103524, <https://doi.org/10.1016/j.arabjc.2021.103524>.
- [65] Z.A. Sahito, A. Zehra, S. Chen, S. Yu, L. Tang, Z. Ali, S. Hamza, M. Irfan, T. Abbas, Z. He, X. Yang, Rhizobium rhizogenes-mediated root proliferation in Cd/Zn hyperaccumulator Sedum alfredii and its effects on plant growth promotion, root exudates and metal uptake efficiency, *J. Hazard Mater.* 424 (2022), 127442, <https://doi.org/10.1016/j.jhazmat.2021.127442>.
- [66] M. Han, K. Maleski, C.E. Shuck, Y. Yang, J.T. Glazar, A.C. Foucher, K. Hantanasirisakul, A. Sarycheva, N.C. Frey, S.J. May, V.B. Shenoy, E.A. Stach, Y. Gogotsi, Tailoring electronic and optical properties of MXenes through forming solid solutions, *J. Am. Chem. Soc.* 142 (2020) 19110–19118, <https://doi.org/10.1021/jacs.0c07395>.
- [67] G. Deysher, C.E. Shuck, K. Hantanasirisakul, N.C. Frey, A.C. Foucher, K. Maleski, A. Sarycheva, V.B. Shenoy, E.A. Stach, B. Anasori, Y. Gogotsi, Synthesis of Mo<sub>4</sub>AlC<sub>4</sub> MAX phase and two-dimensional Mo<sub>4</sub>VC<sub>4</sub> MXene with five atomic layers of transition metals, *ACS Nano* 14 (2020) 204–217, <https://doi.org/10.1021/acsnano.9b07708>.
- [68] M. Naguib, M.W. Barsoum, Y. Gogotsi, Ten years of progress in the synthesis and development of MXenes, *Adv. Mater.* 33 (2021), 2103393, <https://doi.org/10.1002/adma.202103393>.
- [69] M. Khatami, S. Iravani, MXenes and MXene-based materials for the removal of water pollutants: challenges and opportunities, *Comments Mod. Chem.* 41 (2021) 213–248, <https://doi.org/10.1080/02603594.2021.1922396>.
- [70] Y. Sun, Y. Li, Potential environmental applications of MXenes: a critical review, *Chemosphere* 271 (2021), 129578, <https://doi.org/10.1016/j.chemosphere.2021.129578>.
- [71] C. Comanescu, Recent development in nanoconfined hydrides for energy storage, *Int. J. Mol. Sci.* 23 (2022) 7111.
- [72] S. Zhang, M. Bilal, M. Adeel, D. Barceló, H.M.N. Iqbal, MXene-based designer nanomaterials and their exploitation to mitigate hazardous pollutants from environmental matrices, *Chemosphere* 283 (2021), <https://doi.org/10.1016/j.chemosphere.2021.131293>.
- [73] I. Ihsanullah, Potential of MXenes in water desalination: current status and perspectives, *Nano-Micro Lett.* 12 (2020) 1–20, <https://doi.org/10.1007/s40820-020-0411-9>.
- [74] Y. Sheth, S. Dharaskar, V. Chaudhary, M. Khalid, R. Walvekar, Prospects of titanium carbide-based MXene in heavy metal ion and radionuclide adsorption for wastewater remediation: a review, *Chemosphere* 293 (2022), 133563, <https://doi.org/10.1016/j.jchemosphere.2022.133563>.
- [75] I. Ihsanullah, MXenes as next-generation materials for the photocatalytic degradation of pharmaceuticals in water, *J. Environ. Chem. Eng.* 10 (2022), 107381, <https://doi.org/10.1016/j.jece.2022.107381>.
- [76] Ihsanullah, MXenes (two-dimensional metal carbides) as emerging nanomaterials for water purification: Progress, challenges and prospects, *Chem. Eng. J.* (n.d.). <https://doi.org/10.1016/j.cej.2020.124340>.
- [77] I. Ihsanullah, M. Bilal, Potential of MXene-based membranes in water treatment and desalination: a critical review, *Chemosphere* 303 (2022), 135234, <https://doi.org/10.1016/j.chemosphere.2022.135234>.
- [78] J. Zhao, Y. Yang, C. Yang, Y. Tian, Y. Han, J. Liu, X. Yin, W. Que, A hydrophobic surface enabled salt-blocking 2D Ti<sub>3</sub>C<sub>2</sub> MXene membrane for efficient and stable solar desalination, *J. Mater. Chem. A.* 6 (2018) 16196–16204, <https://doi.org/10.1039/C8TA05569F>.
- [79] X. Chen, X. Tong, J. Gao, L. Yang, J. Ren, W. Yang, S. Liu, M. Qi, J. Crittenden, R. Hao, Simultaneous nitrite resorting and mercury ion removal using MXene-anchored goethite heterogeneous fenton composite, *Environ. Sci. Technol.* 56 (2022) 4542–4552, <https://doi.org/10.1021/acs.est.2c00786>.
- [80] Q. Lin, Y. Liu, Z. Yang, Z. He, H. Wang, L. Zhang, M. Belle Marie Yap Ang, G. Zeng, Construction and application of two-dimensional MXene-based membranes for water treatment: a mini-review, *Results Eng* 15 (2022), 100494, <https://doi.org/10.1016/j.rineng.2022.100494>.
- [81] R. Ghanbari, E. Nazarzadeh Zare, A.C. Paiva-Santos, N. Rabiee, Ti<sub>3</sub>C<sub>2</sub>(2)Tx MXene@MOF decorated polyvinylidene fluoride membrane for the remediation of heavy metals ions and desalination, *Chemosphere* 311 (2022), 137191, <https://doi.org/10.1016/j.chemosphere.2022.137191>.
- [82] S. Wang, F. Wang, Y. Jin, X. Meng, B. Meng, N. Yang, J. Sunarso, S. Liu, Removal of heavy metal cations and co-existing anions in simulated wastewater by two separated hydroxylated MXene membranes under an external voltage, *J. Membr. Sci.* 638 (2021), 119697, <https://doi.org/10.1016/j.memsci.2021.119697>.
- [83] X. Xie, C. Chen, N. Zhang, Z. Tang, J. Jiang, Y. Xu, Microstructure and surface control of MXene films for water purification, *Nat. Sustain.* 2 (2019), <https://doi.org/10.1038/s41893-019-0373-4>.
- [84] R. Chen, Y. Cheng, P. Wang, Y. Wang, Q. Wang, Z. Yang, C. Tang, S. Xiang, S. Luo, S. Huang, Facile synthesis of a sandwiched Ti<sub>3</sub>C<sub>2</sub>Tx MXene/nZVI/fungal hypha nanofiber hybrid membrane for enhanced removal of Be (II) from Be (NH<sub>2</sub>)<sub>2</sub> complexing solutions, *J. Chem. Eng.* 421 (2021), 129682, <https://doi.org/10.1016/j.cej.2021.129682>.
- [85] Y. Zhang, S. Zhang, T. Chung, Nanometric graphene oxide framework membranes with enhanced heavy metal removal via nano filtration, *Environ. Sci. Technol.* 49 (2015) 10235–10242, <https://doi.org/10.1021/acs.est.5b02086>.
- [86] X. Zhao, Y. Che, Y. Mo, W. Huang, C. Wang, Fabrication of PEI modified GO/MXene composite membrane and its application in removing metal cations from water, *J. Membr. Sci.* 640 (2021), 119847, <https://doi.org/10.1016/j.memsci.2021.119847>.
- [87] J. Abraham, K.S. Vasu, C.D. Williams, K. Gopinadhan, Y. Su, C.T. Cherian, J. Dix, E. Prestat, S.J. Haigh, I.V. Grigorieva, Tunable sieving of ions using graphene oxide membranes, *Nat. Nanotechnol.* 12 (2017) 546–550, <https://doi.org/10.1038/nnano.2017.21>.
- [88] F. Arshadi, M. Mohammad, E. Hosseini, H. Ahmadi, M. Asadnia, Y. Orooji, A.H. Korayem, A. Noorbakhsh, A. Razmjou, The effect of D-spacing on the ion selectivity performance of MXene membrane, *J. Membr. Sci.* 639 (2021), 119752, <https://doi.org/10.1016/j.memsci.2021.119752>.
- [89] Y. Fan, J. Li, S. Wang, X. Meng, W. Zhang, Y. Jin, N. Yang, X. Tan, J. Li, S. Liu, Voltage-enhanced ion sieving and rejection of Pb<sup>2+</sup> through a thermally cross-linked two-dimensional MXene membrane, *Chem. Eng. J.* 401 (2020), 126073, <https://doi.org/10.1016/j.cej.2020.126073>.
- [90] T.K. Ritter, C.H. Wong, Carbohydrate-based antibiotics: a new approach to tackling the problem of resistance, *Angew. Chem., Int. Ed.* 40 (2001) 3508–3533, [https://doi.org/10.1002/1521-3773\(20011001\)40:19<3508::aid-anie3508>3.0.co;2-i](https://doi.org/10.1002/1521-3773(20011001)40:19<3508::aid-anie3508>3.0.co;2-i).
- [91] T. Brodin, J. Fick, M. Jonsson, J. Klaminder, Dilute concentrations of a psychiatric drug alter behavior of fish from natural populations, *Science* 339 (2013) 814–815, <https://doi.org/10.1126/science.1226850>.
- [92] M. Lakemeyer, W. Zhao, F.A. Mandl, Thinking outside the box-novel antibacterials to tackle the resistance crisis, *Angew. Chem., Int. Ed. Engl.* 57 (2018) 14440–14475, <https://doi.org/10.1002/anie.201804971>.
- [93] R. Zhang, Y. Yang, C.-H. Huang, L. Zhao, P. Sun, Kinetics and modeling of sulfonamide antibiotic degradation in wastewater and human urine by UV/H<sub>2</sub>O<sub>2</sub> and UV/PDS, *Water Res.* 103 (2016) 283–292, <https://doi.org/10.1016/j.watres.2016.07.037>.
- [94] X.Q. Cheng, Y. Liu, Z. Guo, L. Shao, Nanofiltration membrane achieving dual resistance to fouling and chlorine for “green” separation of antibiotics, *J. Membr. Sci.* 493 (2015) 156–166, <https://doi.org/10.1016/j.memsci.2015.06.048>.
- [95] B. Mi, Graphene oxide membranes for ionic and molecular sieving, *Science* 343 (2014) 740–742, <https://doi.org/10.1126/science.1250247>.
- [96] M.A. Shannon, P.W. Bohn, M. Elimelech, J.G. Georgiadis, B.J. Mariñas, A.M. Mayes, Science and technology for water purification in the coming decades, in: *Nanosci. Technol.*, n.d.: pp. 337–346. [https://doi.org/10.1142/9789814287005\\_0035](https://doi.org/10.1142/9789814287005_0035).
- [97] D. Pichardo-Romero, Z.P. Garcia-Arce, A. Zavala-Ramirez, R. Castro-Muñoz, Current advances in biofouling mitigation in membranes for water treatment: an overview, *Processes* 8 (2020) 182, <https://doi.org/10.3390/pr8020182>.

- [98] K. Raidongia, J. Huang, Nanofluidic ion transport through reconstructed layered materials, *J. Am. Chem. Soc.* 134 (2012) 16528–16531, <https://doi.org/10.1021/ja308167f>.
- [99] Q. Yang, Y. Su, C. Chi, C.T. Cherian, K. Huang, V.G. Kravets, F.C. Wang, J.C. Zhang, A. Pratt, A.N. Grigorenko, F. Guinea, A.K. Geim, R.R. Nair, Ultrathin graphene-based membrane with precise molecular sieving and ultrafast solvent permeation, *Nat. Mater.* 16 (2017) 1198–1202, <https://doi.org/10.1038/nmat5025>.
- [100] L. Chen, G. Shi, J. Shen, B. Peng, B. Zhang, Y. Wang, F. Bian, J. Wang, D. Li, Z. Qian, G. Xu, G. Liu, J. Zeng, L. Zhang, Y. Yang, G. Zhou, M. Wu, W. Jin, J. Li, H. Fang, Ion sieving in graphene oxide membranes via cationic control of interlayer spacing, *Nature* 550 (2017) 380–383, <https://doi.org/10.1038/nature24044>.
- [101] Z. Lu, Y. Wei, J. Deng, L. Ding, Z.K. Li, H. Wang, Self-crosslinked MXene (Ti<sub>3</sub>C<sub>2</sub>T<sub>x</sub>) membranes with good anti-swelling property for monovalent metal ion exclusion, *ACS Nano* 13 (2019) 10535–10544, <https://doi.org/10.1021/acsnano.9b04612>.
- [102] Z.-K. Li, Y. Wei, X. Gao, L. Ding, Z. Lu, J. Deng, X. Yang, J. Caro, H. Wang, Antibiotics separation with MXene membranes based on regularly stacked high-aspect-ratio nanosheets, *Angew. Chem., Int. Ed.* 59 (2020) 9751–9756, <https://doi.org/10.1002/anie.202002935>.
- [103] Y. Wang, L. Li, Y. Wei, J. Xue, H. Chen, L. Ding, J. Caro, H. Wang, Water transport with ultralow friction through partially exfoliated g-C<sub>3</sub>N<sub>4</sub> nanosheet membranes with self-supporting spacers, *Angew. Chem., Int. Ed.* 56 (2017) 8974–8980, <https://doi.org/10.1002/anie.201701288>.
- [104] L. Ding, L. Li, Y. Liu, Y. Wu, Z. Lu, J. Deng, Y. Wei, J. Caro, H. Wang, Effective ion sieving with Ti<sub>3</sub>C<sub>2</sub>T<sub>x</sub> MXene membranes for production of drinking water from seawater, *Nat. Sustain.* 3 (2020) 296–302, <https://doi.org/10.1038/s41893-020-0474-0>.
- [105] G. Zeng, Z. He, T. Wan, T. Wang, Z. Yang, Y. Liu, Q. Lin, Y. Wang, A. Sengupta, S. Pu, A self-cleaning photocatalytic composite membrane based on g-C<sub>3</sub>N<sub>4</sub>@MXene nanosheets for the removal of dyes and antibiotics from wastewater, *Separ. Purif. Technol.* 292 (2022), 121037, <https://doi.org/10.1016/j.seppur.2022.121037>.
- [106] H. Zhang, Y. Zheng, H. Zhou, S. Zhu, J. Yang, Nanocellulose-intercalated MXene NF membrane with enhanced swelling resistance for highly efficient antibiotics separation, *Separ. Purif. Technol.* 305 (2023), 122425, <https://doi.org/10.1016/j.seppur.2022.122425>.
- [107] Z. Othman, H.R. Mackey, K.A. Mahmoud, A critical overview of MXenes adsorption behavior toward heavy metals, *Chemosphere* 295 (2022), 133849, <https://doi.org/10.1016/j.chemosphere.2022.133849>.
- [111] Y. Wu, H. Pang, Y. Liu, X. Wang, S. Yu, D. Fu, J. Chen, X. Wang, Environmental remediation of heavy metal ions by novel-nanomaterials: a review, *Environ. Pollut.* 246 (2019) 608–620, <https://doi.org/10.1016/j.envpol.2018.12.076>.
- [112] A. Kayvani, G. Mckay, R. Chamoun, T. Rhadfi, H. Preud, M.A. Atieh, Barium removal from synthetic natural and produced water using MXene as two-dimensional (2-D) nanosheet adsorbent, *Chem. Eng. J.* 317 (2017) 331–342, <https://doi.org/10.1016/j.cej.2017.02.090>.
- [113] S. Kim, F. Gholamirad, M. Yu, C.M. Park, A. Jang, M. Jang, N. Taheri-Qazvini, Y. Yoon, Enhanced adsorption performance for selected pharmaceutical compounds by sonicated Ti<sub>3</sub>C<sub>2</sub>T<sub>x</sub> MXene, *Chem. Eng. J.* 406 (2021), 126789, <https://doi.org/10.1016/j.cej.2020.126789>.
- [114] A.A. Ghani, A. Shahzad, M. Moztahida, K. Tahir, H. Jeon, B. Kim, D.S. Lee, Adsorption and electrochemical regeneration of intercalated Ti<sub>3</sub>C<sub>2</sub>T<sub>x</sub> MXene for the removal of ciprofloxacin from wastewater, *Chem. Eng. J.* 421 (2021), 127780, <https://doi.org/10.1016/j.cej.2020.127780>.
- [115] Y. Feng, H. Wang, J. Xu, X. Du, X. Cheng, Z. Du, H. Wang, Fabrication of MXene/PEI functionalized sodium alginate aerogel and its excellent adsorption behavior for Cr(VI) and Congo Red from aqueous solution, *J. Hazard Mater.* 416 (2021), 125777, <https://doi.org/10.1016/j.jhazmat.2021.125777>.
- [116] P. Karthikeyan, K. Ramkumar, K. Pandi, A. Fayyaz, S. Meenakshi, C.M. Park, Effective removal of Cr(VI) and methyl orange from the aqueous environment using two-dimensional (2D) Ti<sub>3</sub>C<sub>2</sub>T<sub>x</sub> MXene nanosheets, *Ceram. Int.* 47 (2021) 3692–3698, <https://doi.org/10.1016/j.ceramint.2020.09.221>.
- [117] A. Shahzad, M. Nawaz, M. Moztahida, J. Jang, K. Tahir, J. Kim, Y. Lim, V.S. Vassiliadis, S.H. Woo, D.S. Lee, Ti<sub>3</sub>C<sub>2</sub>T<sub>x</sub> MXene core-shell spheres for ultrahigh removal of mercuric ions, *Chem. Eng. J.* 368 (2019) 400–408, <https://doi.org/10.1016/j.cej.2019.02.160>.
- [118] Q. Peng, J. Guo, Q. Zhang, J. Xiang, B. Liu, A. Zhou, R. Liu, Y. Tian, Unique lead adsorption behavior of activated hydroxyl group in two-dimensional titanium carbide, *J. Am. Chem. Soc.* 136 (2014) 3–6.
- [119] Y. Du, B.Y. Ye, L. Wei, Y. Wang, X. Zhang, S. Ye, Efficient removal of Pb(II) by Ti<sub>3</sub>C<sub>2</sub>T<sub>x</sub> powder modified with a silane coupling agent, *J. Mater. Sci.* 54 (2019) 13283–13297.
- [120] X. Feng, Z. Yu, R. Long, X. Li, L. Shao, H. Zeng, G. Zeng, Y. Zuo, Self-assembling 2D/2D (MXene/LDH) materials achieve ultra-high adsorption of heavy metals Ni<sup>2+</sup> through terminal group modification, *Separ. Purif. Technol.* 253 (2020), 117525, <https://doi.org/10.1016/j.seppur.2020.117525>.
- [121] R. Luo, W. Zhang, X. Hu, Y. Liang, J. Fu, M. Liu, F. Deng, Q.-Y. Cao, X. Zhang, Y. Wei, Preparation of sodium ligninsulfonate functionalized MXene using hexachlorocyclotriphosphazene as linkage and its adsorption applications, *Appl. Surf. Sci.* 602 (2022), 154197, <https://doi.org/10.1016/j.apsusc.2022.154197>.
- [122] X. Dao, H. Hao, J. Bi, S. Sun, X. Huang, Surface complexation enhanced adsorption of tetracycline by ALK-MXene, *Ind. Eng. Chem. Res.* 61 (2022) 6028–6036, <https://doi.org/10.1021/acs.iecr.2c00037>.
- [123] S. Sukidpaneend, C. Chawengkijwanich, C. Pokhum, T. Isobe, P. Opaprakasit, P. Sreearunothai, Multi-function adsorbent-photocatalyst MXene-TiO<sub>2</sub> composites for removal of enrofloxacin antibiotic from water, *J. Environ. Sci.* 124 (2023) 414–428, <https://doi.org/10.1016/j.jes.2021.09.042>.
- [124] A. Miri-Jahromi, M. Didandeh, S. Shekarsokhan, Capability of MXene 2D material as an amoxicillin, ampicillin, and cloxacillin adsorbent in wastewater, *J. Mol. Liq.* 351 (2022), 118545, <https://doi.org/10.1016/j.molliq.2022.118545>.
- [125] T. Velempini, E. Prabhakaran, K. Pillay, Recent developments in the use of metal oxides for photocatalytic degradation of pharmaceutical pollutants in water—a review, *Mater. Today Chem.* 19 (2021), 100380, <https://doi.org/10.1016/j.mtchem.2020.100380>.
- [126] S.S. Siwal, K. Sheoran, K. Mishra, H. Kaur, A.K. Saini, V. Saini, D.-V.N. Vo, H.Y. Nezhad, V.K. Thakur, Novel synthesis methods and applications of MXene-based nanomaterials (MBNs) for hazardous pollutants degradation: future perspectives, *Chemosphere* 293 (2022), 133542, <https://doi.org/10.1016/j.chemosphere.2022.133542>.
- [127] S.K. Sharma, A. Kumar, G. Sharma, D.-V.N. Vo, A. García-Peñas, O. Moradi, M. Sillanpää, MXenes based nano-heterojunctions and composites for advanced photocatalytic environmental detoxification and energy conversion: a review, *Chemosphere* 291 (2022), 132923, <https://doi.org/10.1016/j.chemosphere.2021.132923>.
- [128] H. Assad, I. Fatma, A. Kumar, S. Kaya, D.-V.N. Vo, A. Al-Gheethi, A. Sharma, An overview of MXene-Based nanomaterials and their potential applications towards hazardous pollutant adsorption, *Chemosphere* 298 (2022), 134221, <https://doi.org/10.1016/j.chemosphere.2022.134221>.
- [129] S. Cao, B. Shen, T. Tong, J. Fu, J. Yu, 2D/2D heterojunction of ultrathin MXene/Bi<sub>2</sub>WO<sub>6</sub> nanosheets for improved photocatalytic CO<sub>2</sub> reduction, *Adv. Funct. Mater.* 28 (2018), 1800136, <https://doi.org/10.1002/adfm.201800136>.
- [130] B. Anasori, M.R. Lukatskaya, Y. Gogotsi, 2D metal carbides and nitrides (MXenes) for energy storage, *Nat. Rev. Mater.* 2 (2017), <https://doi.org/10.1038/natrevmats.2016.98>.
- [131] J. Nan, X. Guo, J. Xiao, X. Li, W. Chen, W. Wu, H. Liu, Y. Wang, M. Wu, G. Wang, Nanoengineering of 2D MXene-based materials for energy storage applications, *Small* 17 (2021), 1902085, <https://doi.org/10.1002/sml.201902085>.
- [132] M. Li, J. Lu, K. Luo, Y. Li, K. Chang, K. Chen, J. Zhou, J. Rosen, L. Hultman, P. Eklund, P.O.Å. Persson, S. Du, Z. Chai, Z. Huang, Q. Huang, Element replacement approach by reaction with lewis acidic molten salts to synthesize nanolaminated MAX phases and MXenes, *J. Am. Chem. Soc.* 141 (2019) 4730–4737, <https://doi.org/10.1021/jacs.9b00574>.
- [133] O. Salim, K.A. Mahmoud, K.K. Pant, R.K. Joshi, Introduction to MXenes: synthesis and characteristics, *Mater. Today Chem* 14 (2019), 100191, <https://doi.org/10.1016/j.mtchem.2019.08.010>.
- [134] D. Geng, X. Zhao, Z. Chen, W. Sun, W. Fu, J. Chen, W. Liu, W. Zhou, K.P. Loh, Direct synthesis of large-area 2D Mo<sub>2</sub>C on situ grown graphene, *Adv. Mater.* 29 (2017), 1700072, <https://doi.org/10.1002/adma.201700072>.
- [135] C. Xu, L. Wang, Z. Liu, L. Chen, J. Guo, N. Kang, X.-L. Ma, H.-M. Cheng, W. Ren, Large-area high-quality 2D ultrathin Mo<sub>2</sub>C superconducting crystals, *Nat. Mater.* 14 (2015) 1135–1141, <https://doi.org/10.1038/nmat4374>.
- [136] Q. Zhong, Y. Li, G. Zhang, Two-dimensional MXene-based and MXene-derived photocatalysts: recent developments and perspectives, *Chem. Eng. J.* 409 (2021), 128099, <https://doi.org/10.1016/j.cej.2020.128099>.

- [137] Y. Chen, X. Xie, X. Xin, Z.-R. Tang, Y.-J. Xu, Ti3C2Tx-Based three-dimensional hydrogel by a graphene oxide-assisted self-convergence process for enhanced photoredox catalysis, *ACS Nano* 13 (2019) 295–304, <https://doi.org/10.1021/acsnano.8b06136>.
- [138] J.-Y. Li, Y.-H. Li, F. Zhang, Z.-R. Tang, Y.-J. Xu, Visible-light-driven integrated organic synthesis and hydrogen evolution over 1D/2D CdS-Ti3C2Tx MXene composites, *Appl. Catal. B Environ.* 269 (2020), 118783, <https://doi.org/10.1016/j.apcatb.2020.118783>.
- [139] W. Chen, B. Han, Y. Xie, S. Liang, H. Deng, Z. Lin, Ultrathin Co-Co LDHs nanosheets assembled vertically on MXene: 3D nanoarrays for boosted visible-light-driven CO2 reduction, *Chem. Eng. J.* 391 (2020), 123519, <https://doi.org/10.1016/j.cej.2019.123519>.
- [140] P. Kuang, J. Low, B. Cheng, J. Yu, J. Fan, MXene-based photocatalysts, *J. Mater. Sci. Technol.* 56 (2020) 18–44, <https://doi.org/10.1016/j.jmst.2020.02.037>.
- [141] Y. Cao, Y. Fang, X. Lei, B. Tan, X. Hu, B. Liu, Q. Chen, Fabrication of novel CuFe2O4/MXene hierarchical heterostructures for enhanced photocatalytic degradation of sulfonamides under visible light, *J. Hazard Mater.* 387 (2020), 122021, <https://doi.org/10.1016/j.jhazmat.2020.122021>.
- [142] S. Irvani, R.S. Varma, MXene-based photocatalysts in degradation of organic and pharmaceutical pollutants, *Molecules* 27 (2022), <https://doi.org/10.3390/molecules27206939>.
- [143] A. Javaid, S. Latif, M. Imran, N. Hussain, M. Bilal, H.M.N. Iqbal, MXene-based hybrid composites as photocatalyst for the mitigation of pharmaceuticals, *Chemosphere* 291 (2022), 133062, <https://doi.org/10.1016/j.chemosphere.2021.133062>.
- [144] N. Saafie, M. Zulfikar, M.F.R. Samsudin, S. Sufian, Current scenario of MXene-based nanomaterials for wastewater remediation: a review, *Chemistry* 4 (2022) 1576–1608, <https://doi.org/10.3390/chemistry4041014>.
- [145] X. Feng, Z. Yu, Y. Sun, R. Long, M. Shan, X. Li, Y. Liu, J. Liu, Review MXenes as a new type of nanomaterial for environmental applications in the photocatalytic degradation of water pollutants, *Ceram. Int.* 47 (2021) 7321–7343, <https://doi.org/10.1016/j.ceramint.2020.11.151>.
- [146] T. Wojciechowski, A. Rozmysłowska-Wojciechowska, G. Matyszczyk, M. Wrzecieć, A. Olszyna, A. Peter, A. Mihaly-Cozmuta, C. Nicula, L. Mihaly-Cozmuta, S. Podsiadło, D. Basiak, W. Ziemkowska, A. Jastrzębska, Ti2C MXene modified with ceramic oxide and noble metal nanoparticles: synthesis, morphostructural properties, and high photocatalytic activity, *Inorg. Chem.* 58 (2019) 7602–7614, <https://doi.org/10.1021/acs.inorgchem.9b01015>.
- [147] L.C. Makola, S. Moeno, C.N.M. Ouma, A. Sharma, D.-V.N. Vo, L.N. Dlamini, Facile fabrication of a metal-free 2D–2D Nb2CTx@g-C3N4 MXene-based Schottky-heterojunction with the potential application in photocatalytic processes, *J. Alloys Compd.* 916 (2022), 165459, <https://doi.org/10.1016/j.jallcom.2022.165459>.
- [148] J. Wang, R. Zhuan, L. Chu, The occurrence, distribution and degradation of antibiotics by ionizing radiation: an overview, *Sci. Total Environ.* 646 (2019) 1385–1397, <https://doi.org/10.1016/j.scitotenv.2018.07.415>.
- [149] L. Lu, Q. Yang, Q. Xu, Y. Sun, S. Tang, X. Tang, H. Liang, Y. Yu, Two-dimensional materials beyond graphene for the detection and removal of antibiotics: a critical review, *Crit. Rev. Environ. Sci. Technol.* 52 (2022) 3493–3524, <https://doi.org/10.1080/10643389.2021.1929001>.
- [150] Y. Wu, X. Li, Q. Yang, D. Wang, F. Yao, J. Cao, Z. Chen, X. Huang, Y. Yang, X. Li, Mxene-modulated dual-heterojunction generation on a metal-organic framework (MOF) via surface constitution reconstruction for enhanced photocatalytic activity, *Chem. Eng. J.* 390 (2020), 124519, <https://doi.org/10.1016/j.cej.2020.124519>.
- [151] A. Shahzad, K. Rasool, M. Nawaz, W. Miran, J. Jang, M. Moztahida, K.A. Mahmoud, D.S. Lee, Heterostructural TiO2/Ti3C2Tx (MXene) for photocatalytic degradation of antiepileptic drug carbamazepine, *Chem. Eng. J.* 349 (2018) 748–755, <https://doi.org/10.1016/j.cej.2018.05.148>.
- [152] Q. Liu, X. Tan, S. Wang, F. Ma, H. Znad, Z. Shen, L. Liu, S. Liu, MXene as a non-metal charge mediator in 2D layered CdS@Ti3C2Tx/TiO2 composites with superior Z-scheme visible light-driven photocatalytic activity, *Environ. Sci. Nano.* 6 (2019) 3158–3169, <https://doi.org/10.1039/C9EN00567F>.
- [153] X. Yi, J. Yuan, H. Tang, Y. Du, B. Hassan, K. Yin, Y. Chen, X. Liu, Embedding few-layer Ti3C2Tx into alkalized g-C3N4 nanosheets for efficient photocatalytic degradation, *J. Colloid Interface Sci.* 571 (2020) 297–306, <https://doi.org/10.1016/j.jcis.2020.03.061>.
- [154] J. Jang, A. Shahzad, S.H. Woo, D.S. Lee, Magnetic Ti3C2Tx (MXene) for diclofenac degradation via the ultraviolet/chlorine advanced oxidation process, *Environ. Res.* 182 (2020), 108990, <https://doi.org/10.1016/j.envres.2019.108990>.
- [155] X. Zou, X. Zhao, J. Zhang, W. Lv, L. Qiu, Z. Zhang, Photocatalytic degradation of ranitidine and reduction of nitrosamine dimethylamine formation potential over MXene–Ti3C2/MoS2 under visible light irradiation, *J. Hazard Mater.* 413 (2021), 125424, <https://doi.org/10.1016/j.jhazmat.2021.125424>.
- [156] H. Liu, C. Yang, X. Jin, J. Zhong, J. Li, One-pot hydrothermal synthesis of MXene Ti3C2/TiO2/BiOCl ternary heterojunctions with improved separation of photoactivated carries and photocatalytic behavior toward elimination of contaminants, *Colloids Surfaces A Physicochem. Eng. Asp.* 603 (2020), 125239, <https://doi.org/10.1016/j.colsurfa.2020.125239>.
- [157] W. Liu, M. Sun, Z. Ding, B. Gao, W. Ding, Ti3C2 MXene embellished g-C3N4 nanosheets for improving photocatalytic redox capacity, *J. Alloys Compd.* 877 (2021), 160223, <https://doi.org/10.1016/j.jallcom.2021.160223>.
- [158] Y. Ma, D. Xu, W. Chen, Y. Tang, X. Wang, L. Li, J. Wang, Oxygen-vacancy-embedded 2D/2D NiFe-LDH/MXene Schottky heterojunction for boosted photodegradation of norfloxacin, *Appl. Surf. Sci.* 572 (2022), 151432, <https://doi.org/10.1016/j.apsusc.2021.151432>.
- [159] L. Cheng, G. Liu, J. Zhao, W. Jin, Two-dimensional-material membranes: manipulating the transport pathway for molecular separation, *Accounts Mater. Res.* 2 (2021) 114–128, <https://doi.org/10.1021/accountsmr.0c00092>.
- [160] K. Varoon, X. Zhang, B. Elyassi, D.D. Brewer, M. Gettel, S. Kumar, J. Lee, S. Maheshwari, A. Mittal, C. Sung, M. Cococcioni, L. Franxis, A. McCormick, K. Mkhoyan, M. Tsapatsis, Dispersible exfoliated zeolite nanosheets and their application as a selective membrane, *Science* 334 (2011) 72–75.
- [161] Y. Peng, Y. Li, Y. Ban, H. Jin, W. Jiao, X. Liu, W. Yang, Metal-organic framework nanosheets as building blocks for molecular sieving membranes, *Science* 346 (2014) 1356–1359.
- [162] R. Li, Y. Ren, P. Zhao, J. Wang, J. Liu, Y. Zhang, Graphitic carbon nitride (g-C(3)N(4)) nanosheets functionalized composite membrane with self-cleaning and antibacterial performance, *J. Hazard Mater.* 365 (2019) 606–614, <https://doi.org/10.1016/j.jhazmat.2018.11.033>.
- [163] J. Zhu, J. Hou, A. Uliana, Y. Zhang, M. Tian, B. Van Der Bruggen, The rapid emergence of two-dimensional nanomaterials for high-performance separation membranes, *J. Mater. Chem. A* 6 (2018) 3773–3792, <https://doi.org/10.1039/c7ta10814a>.
- [164] P.O. Oviroh, T.-C. Jen, J. Ren, L.M. Mohlala, R. Warmbier, S. Karimzadeh, Nanoporous MoS2 membrane for water desalination: a molecular dynamics study, *Langmuir* 37 (2021) 7127–7137, <https://doi.org/10.1021/acs.langmuir.1c00708>.
- [165] X. Sui, Z. Yuan, Y. Yu, K. Goh, Y. Chen, 2D material based advanced membranes for separations in organic solvents, *Small* 16 (2020), 2003400, <https://doi.org/10.1002/smll.202003400>.
- [166] S.-J. Gao, H. Qin, P. Liu, J. Jin, SWCNT-intercalated GO ultrathin films for ultrafast separation of molecules, *J. Mater. Chem. A* 3 (2015) 6649–6654, <https://doi.org/10.1039/C5TA00366K>.
- [167] L. Ding, Y. Wei, Y. Wang, H. Chen, J. Caro, H. Wang, A two-dimensional lamellar membrane: MXene nanosheet stacks, *Angew. Chem. Int. Ed.* 56 (2017) 1825–1829, <https://doi.org/10.1002/anie.201609306>.
- [168] H. Huang, Y. Mao, Y. Ying, Y. Liu, L. Sun, X. Peng, Salt concentration, pH and pressure controlled separation of small molecules through lamellar graphene oxide membranes, *Chem. Commun.* 49 (2013) 5963–5965, <https://doi.org/10.1039/C3CC41953C>.
- [169] L. Sun, H. Huang, X. Peng, Lamellar MoS2 membranes for molecule separation, *Chem. Commun.* 49 (2013) 10718–10720, <https://doi.org/10.1039/C3CC46136J>.
- [170] L. Sun, Y. Ying, H. Huang, Z. Song, Y. Mao, Z. Xu, X. Peng, Ultrafast molecule separation through layered WS2 nanosheet membranes, *ACS Nano* 8 (2014) 6304–6311, <https://doi.org/10.1021/nn501786m>.
- [171] P. Li, Y.-X. Li, Y.-Z. Wu, Z.-L. Xu, H.-Z. Zhang, P. Gao, S.-J. Xu, Thin-film nanocomposite NF membrane with GO on macroporous hollow fiber ceramic substrate for efficient heavy metals removal, *Environ. Res.* 197 (2021), 111040, <https://doi.org/10.1016/j.envres.2021.111040>.

- [172] M. Sreeramreddygari, J. Mannekote Shivanna, M. Somasundrum, K. Soontarapa, W. Surareungchai, Polythiocyanuric acid-functionalized MoS<sub>2</sub> nanosheet-based high flux membranes for removal of toxic heavy metal ions and Congo red, *Chem. Eng. J.* 425 (2021), 130592, <https://doi.org/10.1016/j.cej.2021.130592>.
- [173] M.M. Tunesi, R.A. Soomro, X. Han, Q. Zhu, Y. Wei, B. Xu, Application of MXenes in environmental remediation technologies, *Nano Converge* 8 (2021) 5, <https://doi.org/10.1186/s40580-021-00255-w>.
- [174] J.A. Kumar, P. Prakash, T. Krithiga, D.J. Amarnath, J. Premkumar, N. Rajamohan, Y. Vasseghian, P. Saravanan, M. Rajasimman, Methods of synthesis, characteristics, and environmental applications of MXene: a comprehensive review, *Chemosphere* 286 (2022), 131607, <https://doi.org/10.1016/j.chemosphere.2021.131607>.